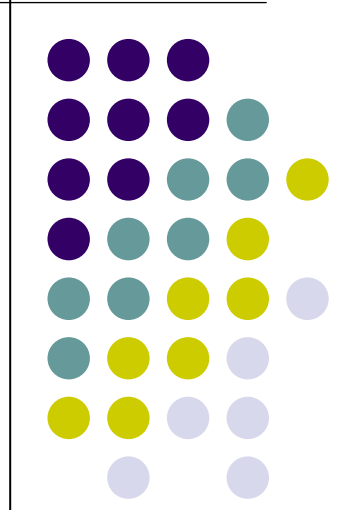
Gold-Nanoparticle-Based Nanophotonics and Bioelectronics

Shangjr Gwo (果尚志)

NATIONAL TSING-HUA UNIVERSITY
DEPARTMENT OF PHYSICS

Hsinchu 300, Taiwan

E-mail: gwo@phys.nthu.edu.tw



2007年日本京都大學-台灣清華大學材料論壇 December 17-18, 2007

Acknowledgments

Collaborators:

陳力俊教授 (Prof. Lih-Juann, NTHU) — Nanoparticles 林寬鋸教授 (Prof. Kuan-Jiuh, NCHU) — Nanoparticles, FTIR 杉村博之教授 (Prof. Hiroyuki Sugimura, Kyoto Univ.)

- SAM

Ph.D. Students:

曾賢德 (Dr. S.-D.Tzeng, Assistant Professor at National

Chung-Hsing Univ.) — EFM, Nanoparticles

陳季汎 (C.-F. Chen) — MEC, Nanoparticle Plasmonic Crystals

林孟賢 (M.-S. Lin) — MEC, SAM

邱繼舜 (C.-S. Chiu) — SAW

陳虹穎 (H.-Y. Chen) — μ -PL and μ -Extinction

Funding:

National Science Council
National Nanoscience and Technology Project



Outline

Motivation:

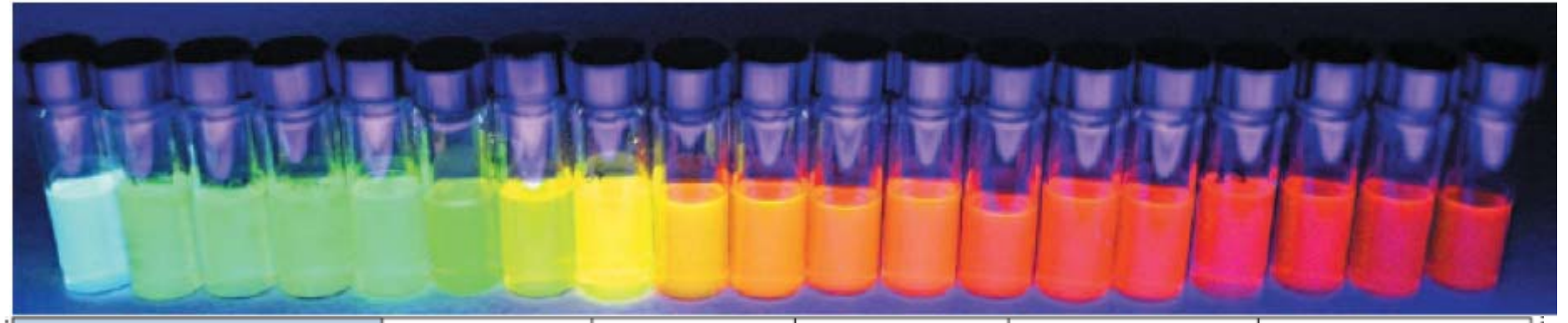
Nanoparticles (especially colloidal nanoparticles) and nanowires are important building blocks for nanotechnology due to their unique size effects and tunable material properties.

- → Controlled assembly using patterned charge-trapping media or self-assembled monolayers for manipulation of nanomaterials
- → Self-Assembled macro-structures showing collective properties of nanomaterials
- Serial electrostatic assembly of thiol-terminated gold and CdSe/ZnS nanoparticles
- → Electrostatic Force Microscopy (**EFM**), <u>Ultra-high-resolution (30 nm)</u>, <u>Possibility of hierarchical assembly</u>
- Parallel electrostatic assembly of 2D nanoparticle arrays via the microcontact electrochemical conversion (MEC) process
- → Multiple length scales (nm, μm, mm, to cm), Rapid/scalable process
- Self-Assembly of alkanethiolate-stabilized gold nanoparticle superlattices (monolayers of hexagonal close-packed nanoparticle
- Demonstration of "nanoparticle plasmonic crystals" with tunable optical properties

CdSe/ZnS Core-Shell Nanoparticleby Bottom-Up Colloidal Chemistry

http://www.evidenttech.com/ Evident Technologies



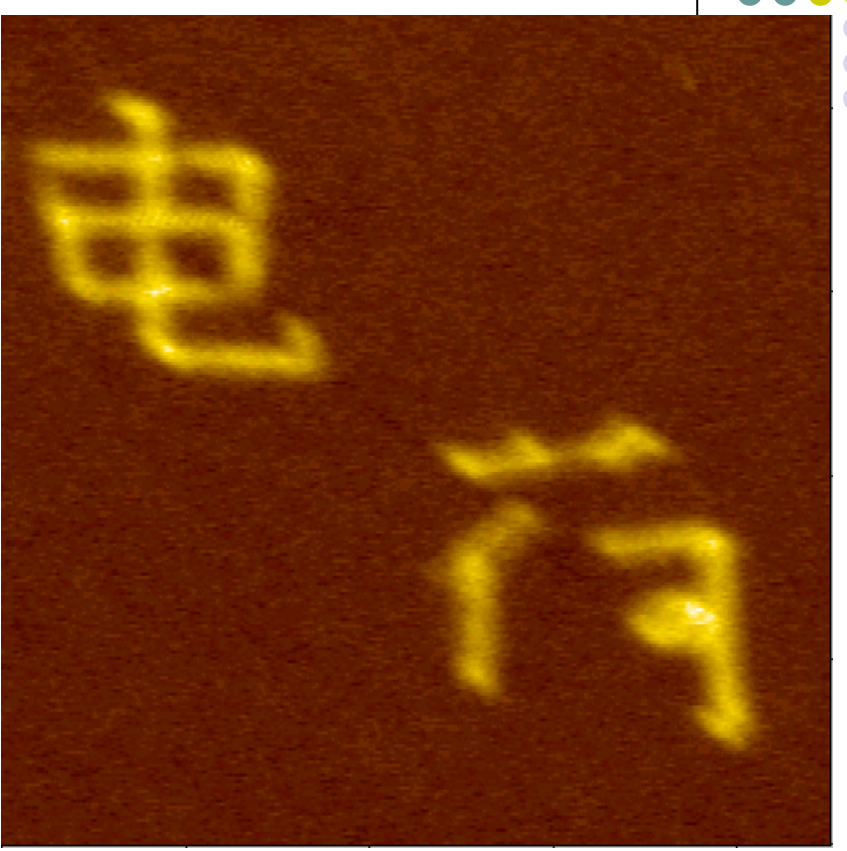


Color	Green	Yellow	Orange	Red-Orange	Red
r · · · · · · · · · · · · · · · · · · ·	525 42	560.40	505.10	(12.12	610.10
Emission Peak [nm]	535±10	560±10	585±10	610±10	640±10
Typical FWHM [nm]	<30	<30	<30	<30	<40
1st Exciton Peak [nm - nominal]	522	547	572	597	627
Crystal Diameter [nm - nominal]	2.8	3.4	4.0	4.7	5.6

Charge-Based Nanomanipulation





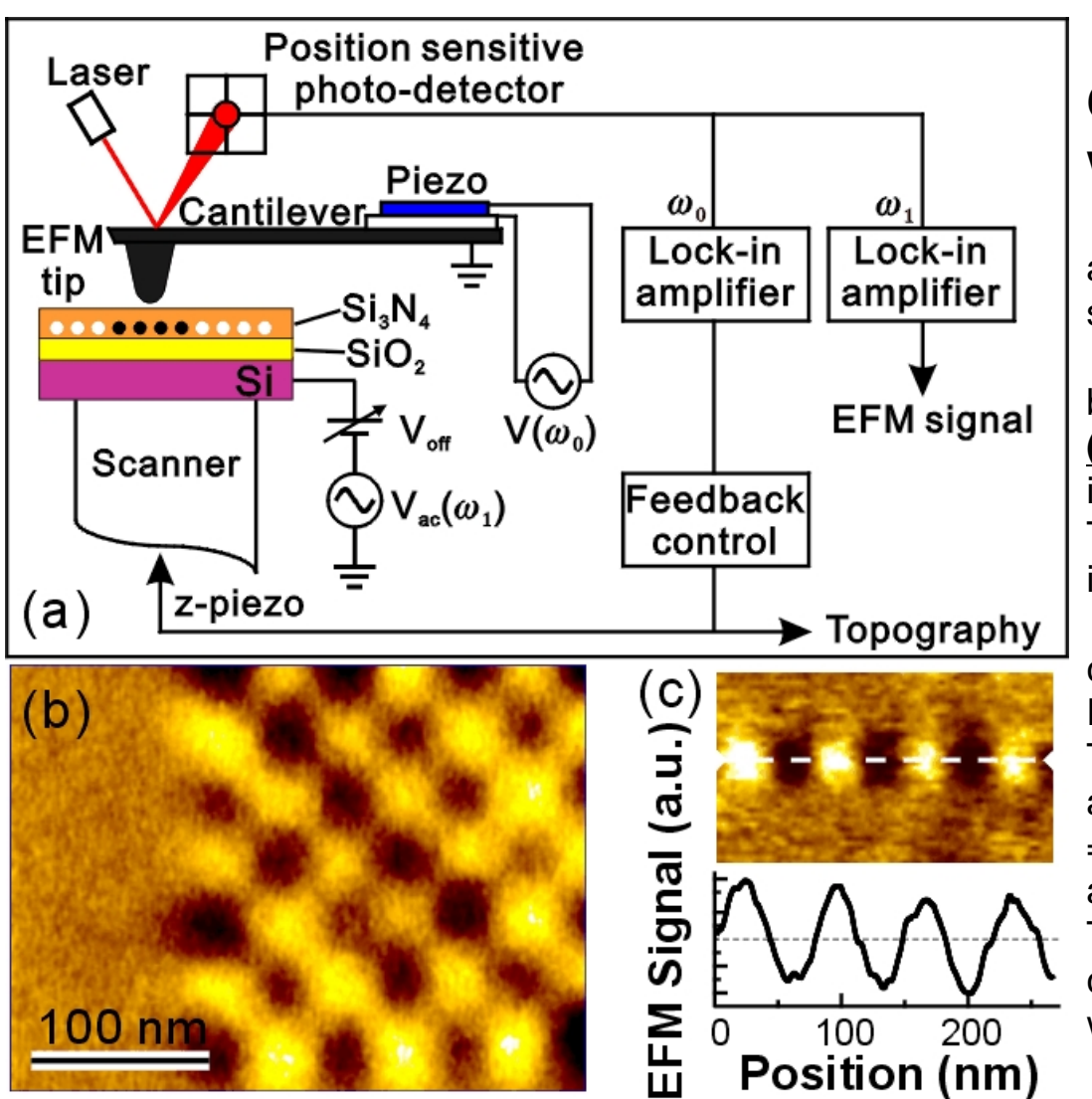


Writing speed: 20 µm/s Sample bias: +4.0 V

Area: 5 µm²

Writing speed: 20 µm/s Sample bias: -4.5 V

Area: $5 \mu m^2$

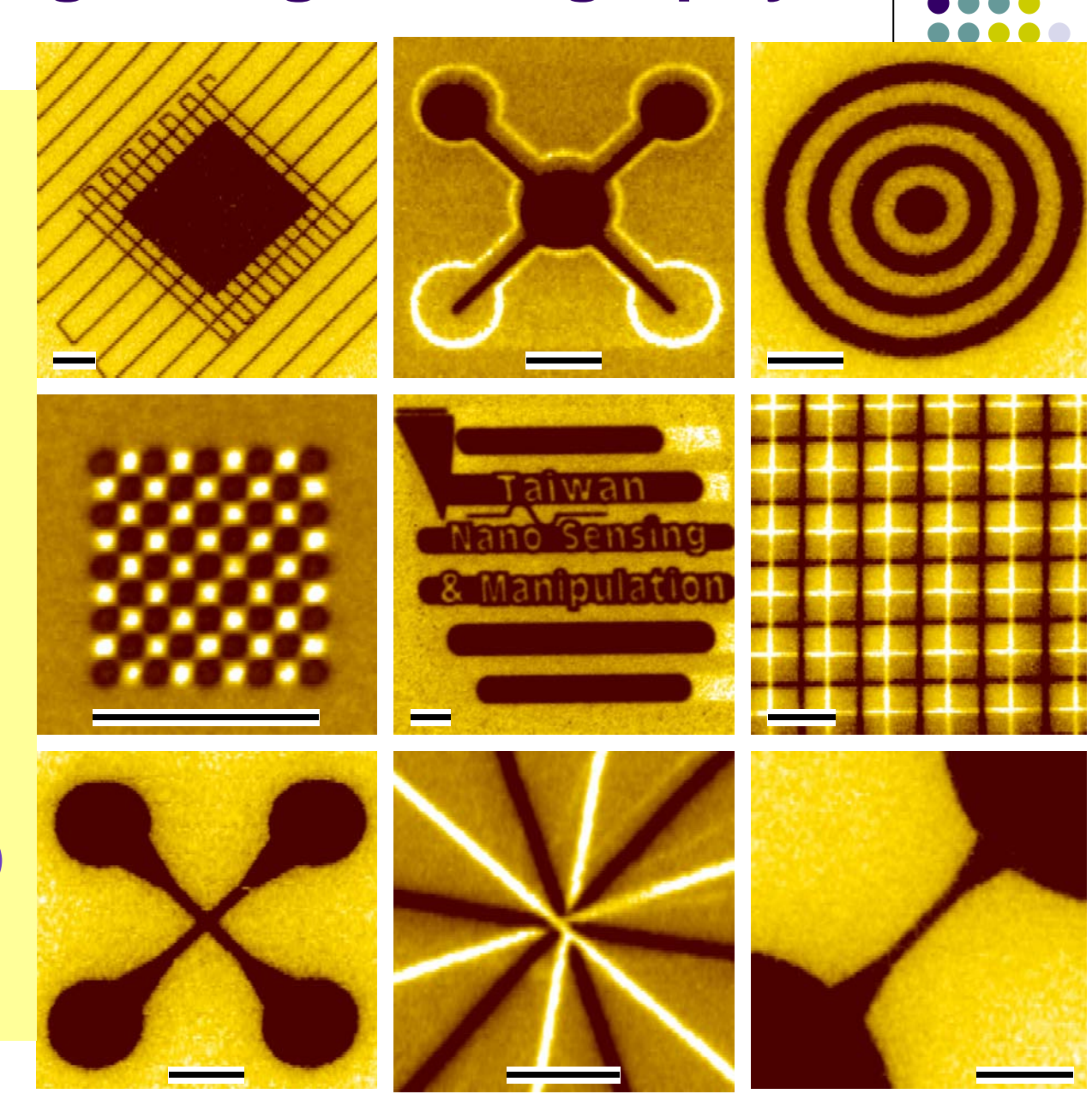


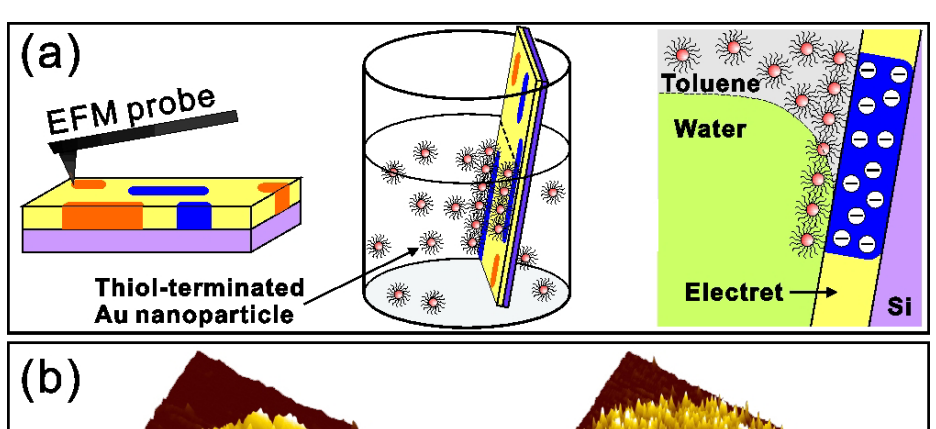
Charge sensing and manipulation with nanoscale resolution

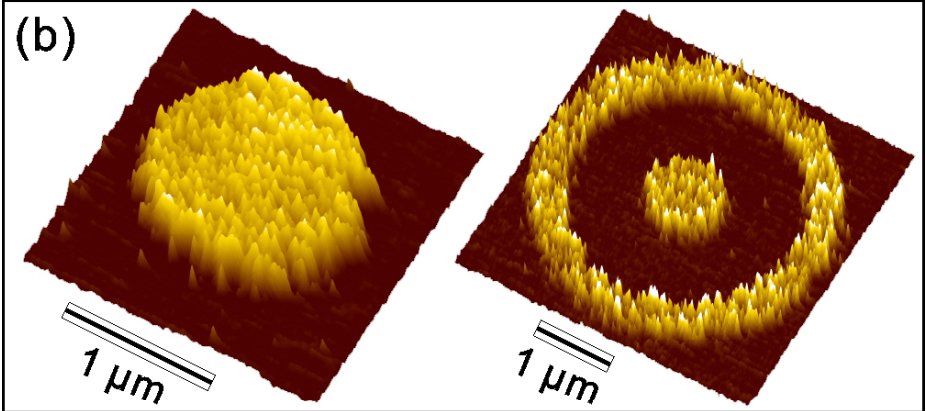
- a) Schematic drawing of the charge sensing and manipulation set-up.
- b) EFM images of high areal density (~500 Gbit/in²) charge bits injected into an NOS (30 Å/22 Å) ultrathin film. The darker and brighter regions were injected with electrons and holes.
- c) EFM image and cross-sectional EFM line profile of charge bits. These charge bits were written by a ± 10 V square wave (repetition rate = 60 kHz) on NOS (30 Å/22 Å) with a tip moving speed of ~ 4.3 mm/s. These results show that charge bits can be written in less than 10 μ s with a minimum feature size of ~ 30 nm.
- 1. S.-D. Tzeng et al., Adv. Mater. 18, 1147-1151 (2006)
- 2. S.-D. Tzeng and S. Gwo, J. Appl. Phys. 100, 023711 (2006)

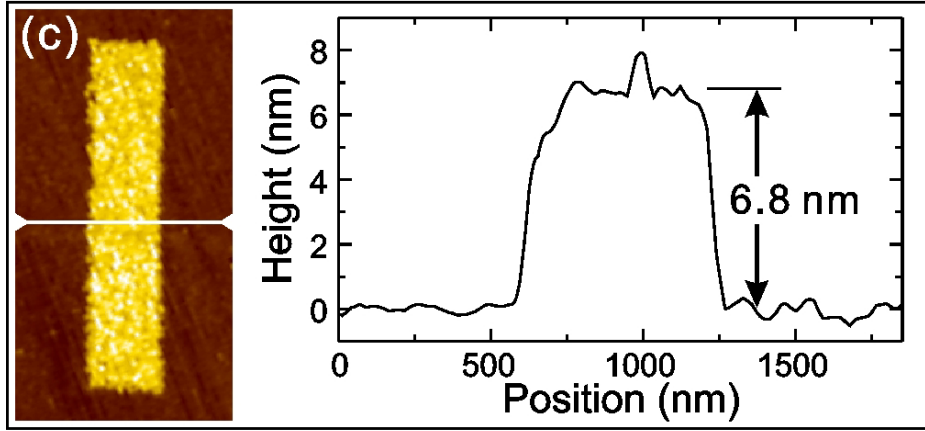
Scanning Charge Lithography

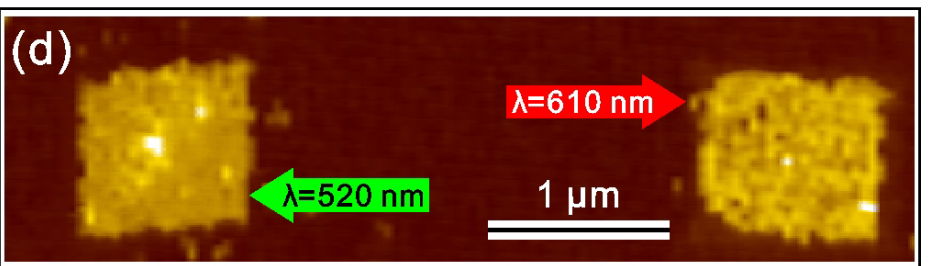
- High resolution (~30 nm)
- High speed (tunneling-based process)
- Erasable/ Rewritable
- Long retention time
- Robust (<u>liquid</u>, gas, and ambient)
- Scalable (nm to cm)









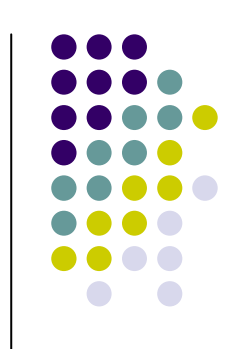


Shien-Der Tzeng, Kuan-Jiuh Lin, Jung-Chih Hu, Lih-Juann Chen, and Shangir Gwo, *Adv. Mater. 18*, 1147-1151 (2006)

Selective adsorption of <u>thiol-terminated</u> gold and CdSe/ZnS nanoparticles.

- a) Schematic of three steps to perform selective adsorption of gold colloidal nanoparticles in a toluene solution using electrostatic patterns created on Si₃N₄/SiO₂/Si electret.
- b) 3D AFM images of selectively adsorbed gold nanoparticles.
- c) Cross-sectional topographic height of selectively adsorbed gold nanoparticles, showing that only a monolayer of close-packed nanoparticles can be formed on the negatively charged surface regions.
- d) AFM image of selectively adsorbed CdSe/ZnS core-shell nanoparticles. Two kinds of thiol-terminated CdSe/ZnS nanoparticles, corresponding to PL wavelengths of ~610 nm (red) and ~520 nm (green) were successively adsorbed by repeating the selective adsorption procedure at different sample areas.

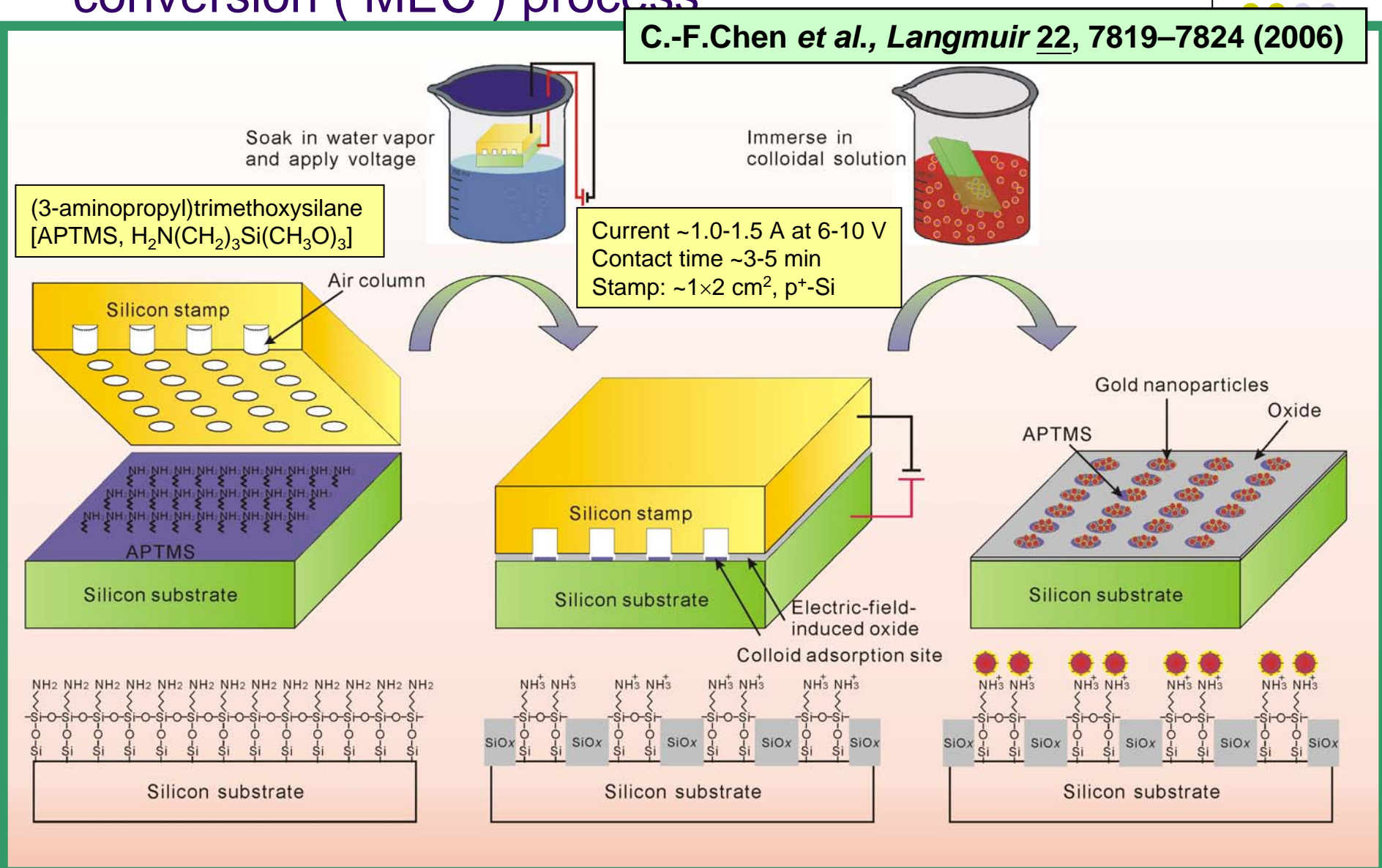
Charge state of thiol-terminated Au nanoparticles in toluene



- Dodecanethiol (C₁₂H₂₅SH)-terminated, 5-nm-diameter gold nanoparticles are suspended in toluene.
- The positive surface charge is related to the TOA+ surfactant used to transfer the nanoparticles from water to toulene.

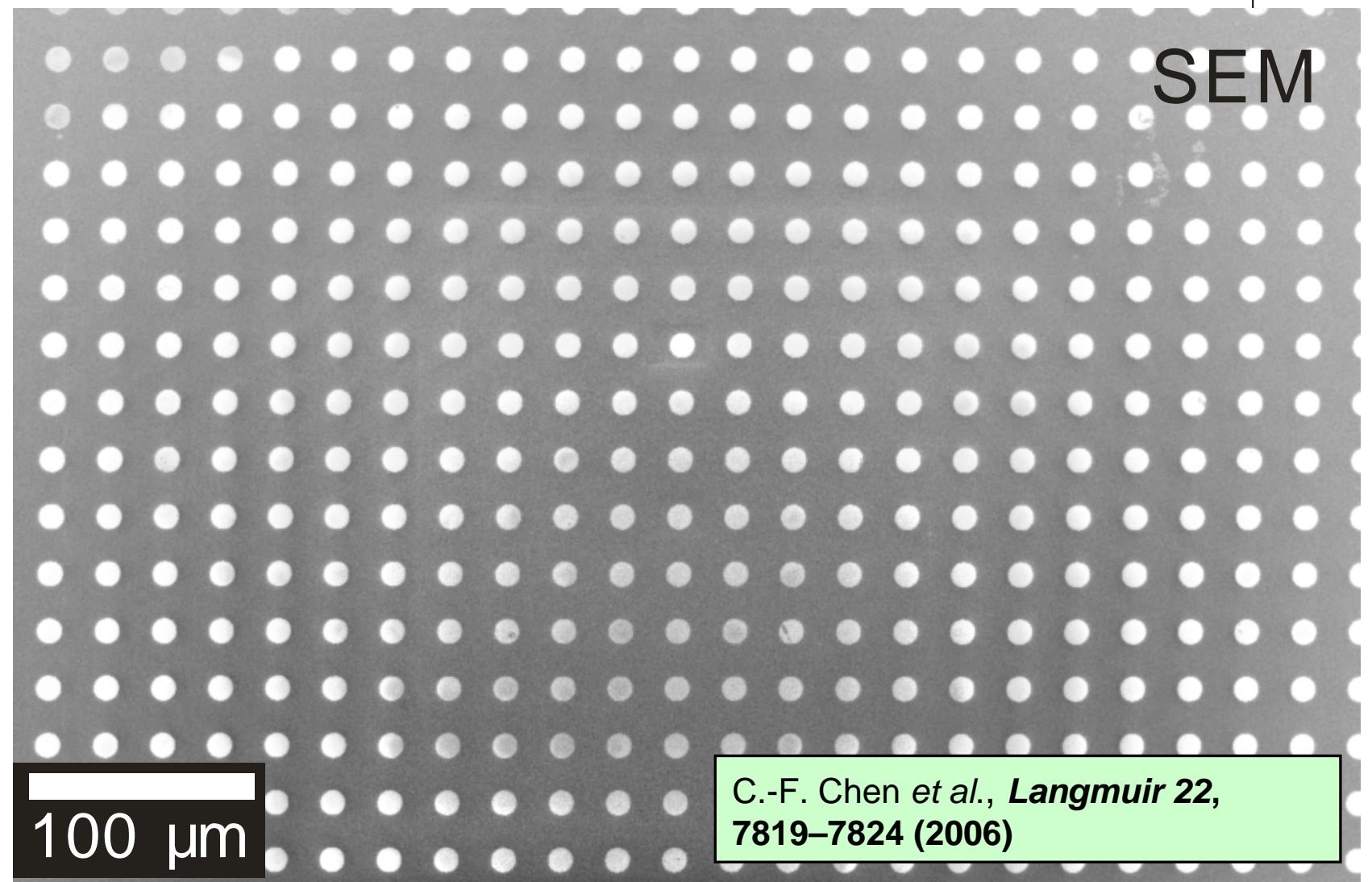
TOAB: tetraoctylammonium bromide [(C₈H₁₇)₄NBr, phase transfer agent]

Parallel electrostatic assembly of 2D nanoparticle arrays via the microcontact electrochemical conversion (MEC) process

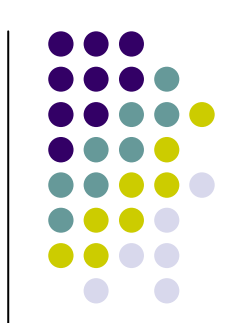


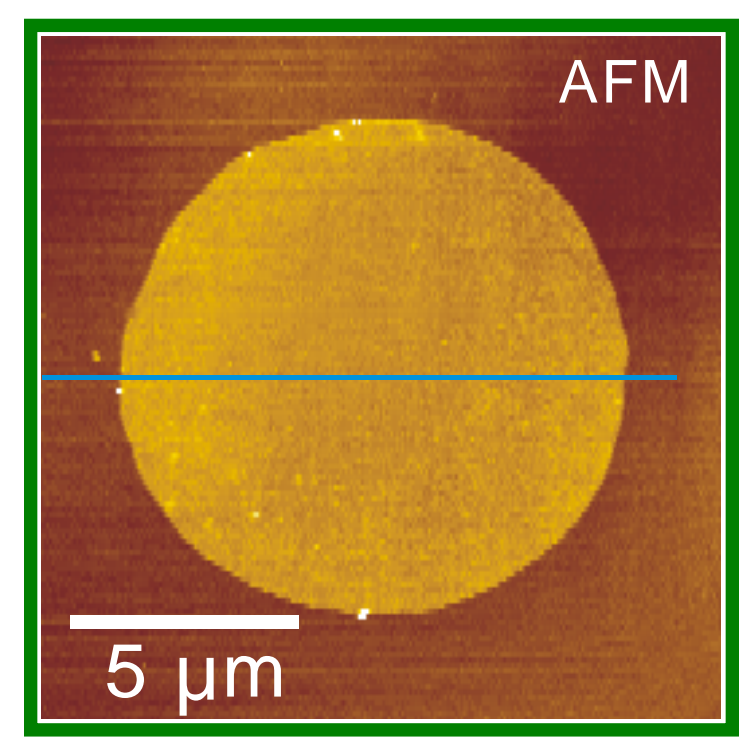
Scanning electron microscopy (SEM) image of large-area oxide pattern created by MEC



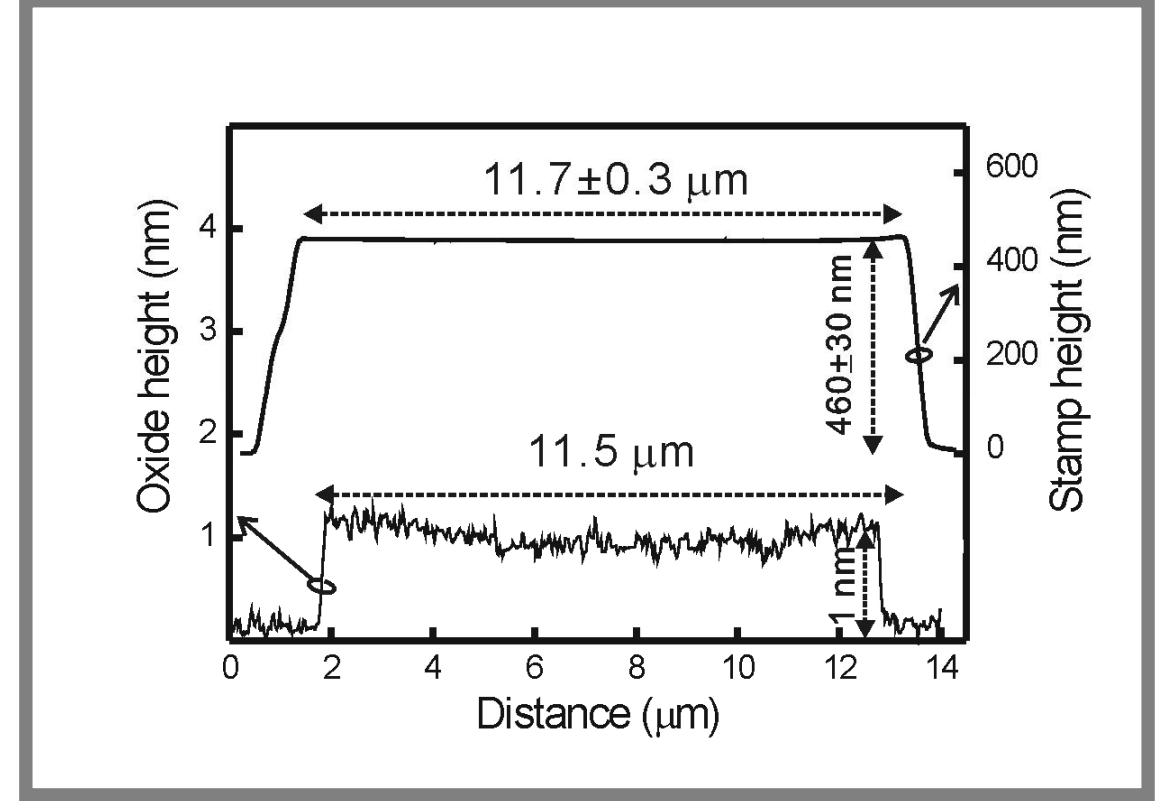


Atomic force microscopy (AFM) topographic image of a single oxide disk and AFM line profiles of the silicon microcontact stamp and the resulting oxide pattern





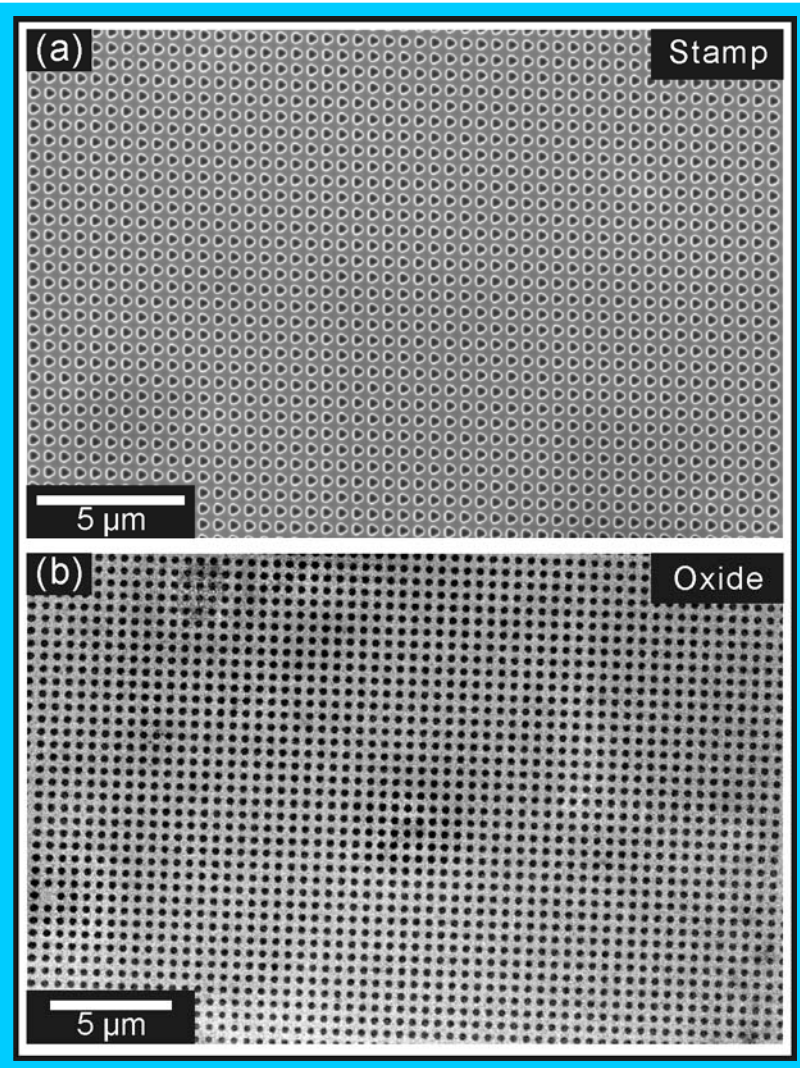
Atomic force microscopy (AFM) topographic image of a single oxide disk.



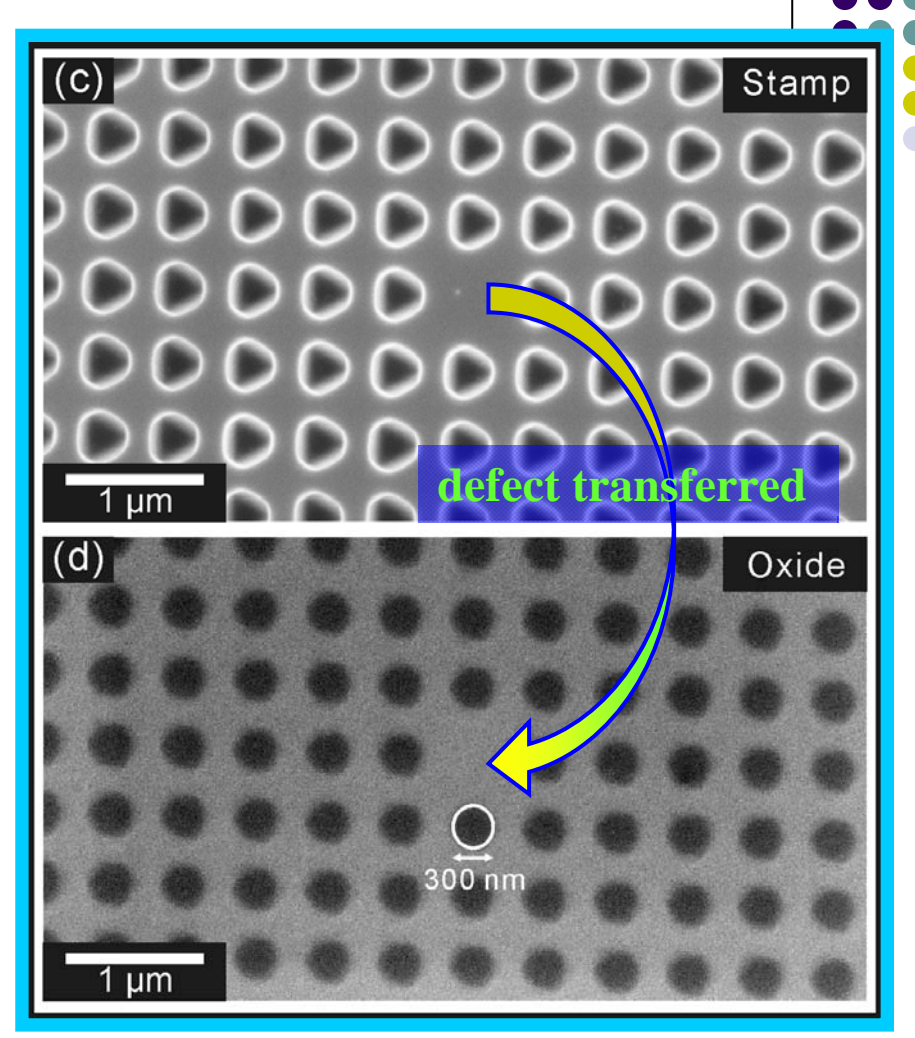
AFM line profiles of the silicon microcontact stamp and the resulting oxide pattern. The lateral dimension of the silicon cylinders on the stamp is given by the mean diameter measured from six Si disks.

C.-F.Chen et al., Langmuir 22, 7819-7824 (2006)

Negative-type MEC pattern transfer

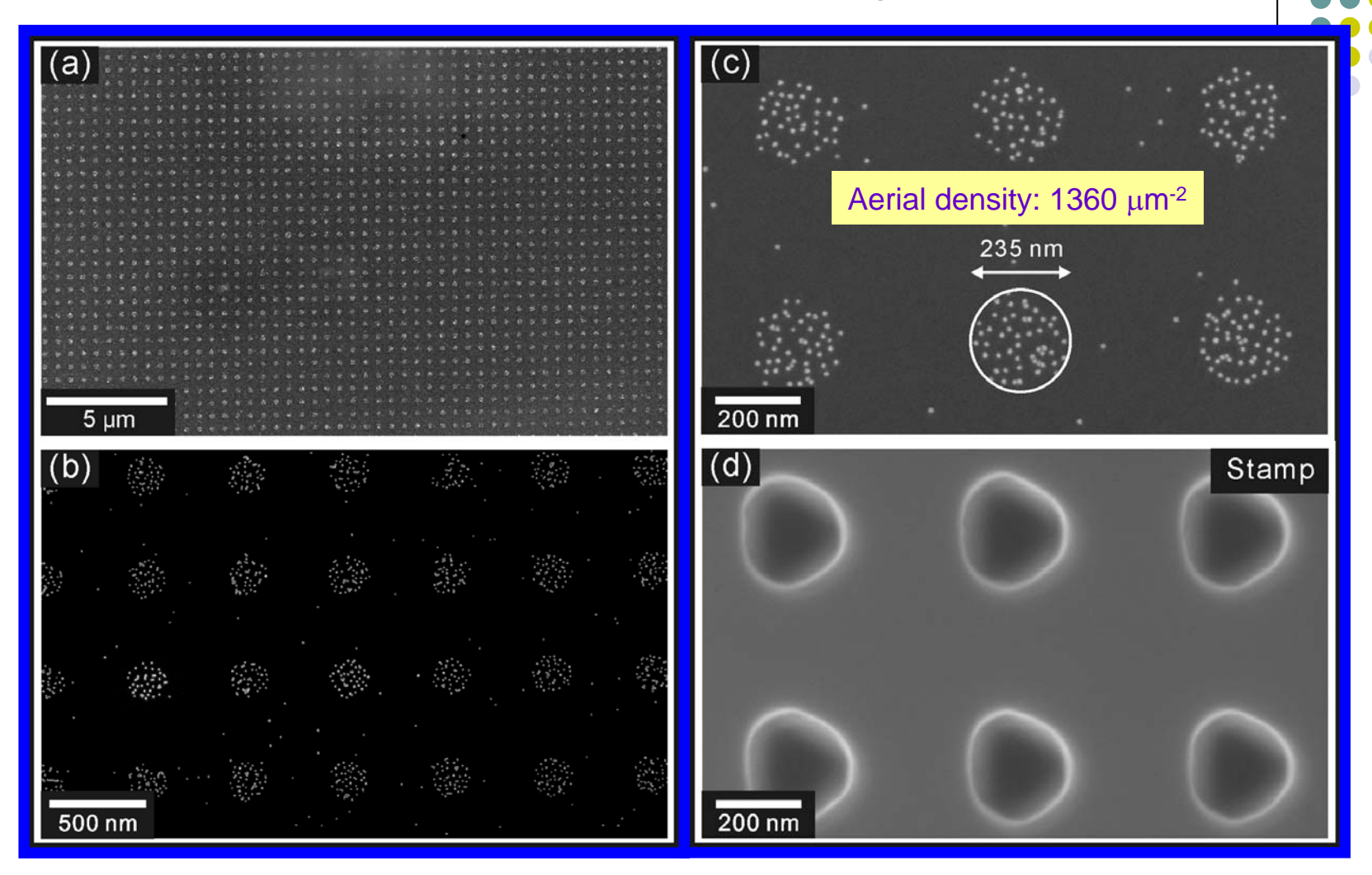


(a) Large-area SEM image of a negativetype Si MEC stamp; (b) Large-area SEM image of an oxide pattern created by the MEC process on a Si substrate;



- (c) High-magnification SEM image of the stamp;
- (d) High-magnification SEM image of the corresponding oxide pattern after the MEC process. The defect on the stamp is faithfully transferred to the oxide pattern.

SEM images of site-controlled adsorption of Au nanoparticle arrays



(a-c) The Si substrate is preassembled with an APTMS monolayer before the MEC process. 99% of Au nanoparticles are selectively adsorbed on the MEC-defined adsorption sites. (d) SEM image of the Si MEC stamp used for creating the nanoparticle adsorption template.



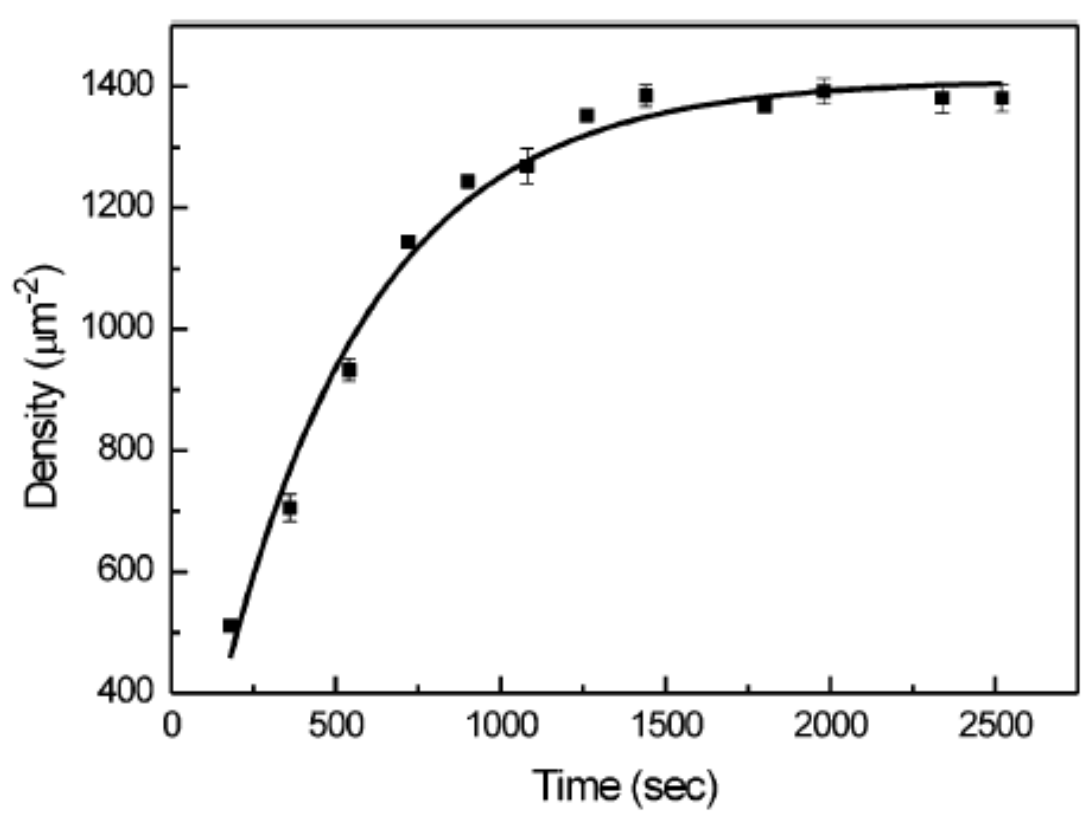
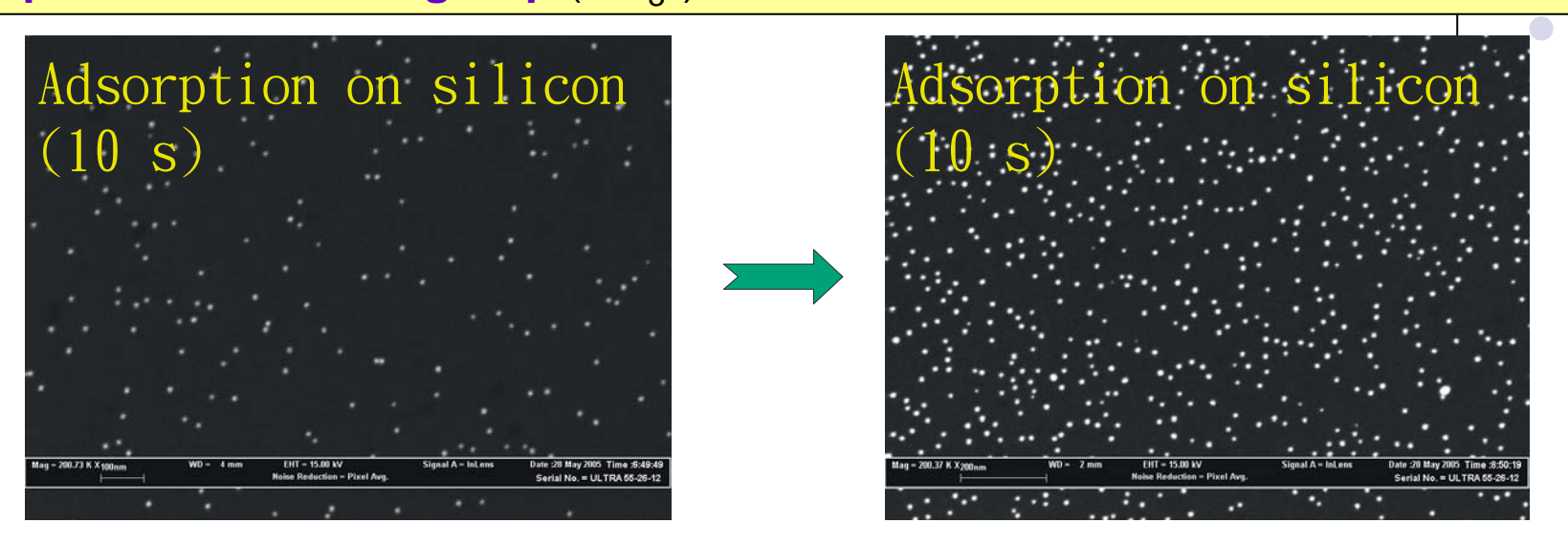


Figure 4. SEM images are used to quantify the extent of colloidal nanoparticle adsorption onto unpatterned, pristine APTMS SAMs. The number of Au nanoparticles per square micrometer (average \pm standard deviation) is obtained by counting nanoparticles in five different areas (1.5 \times 1.5 square micrometer). From a series of related experiments, we find that the nanoparticle adsorption rate drops exponentially with the immersion time and eventually reaches zero at a saturation nanoparticle density (as indicated by the fitting curve).

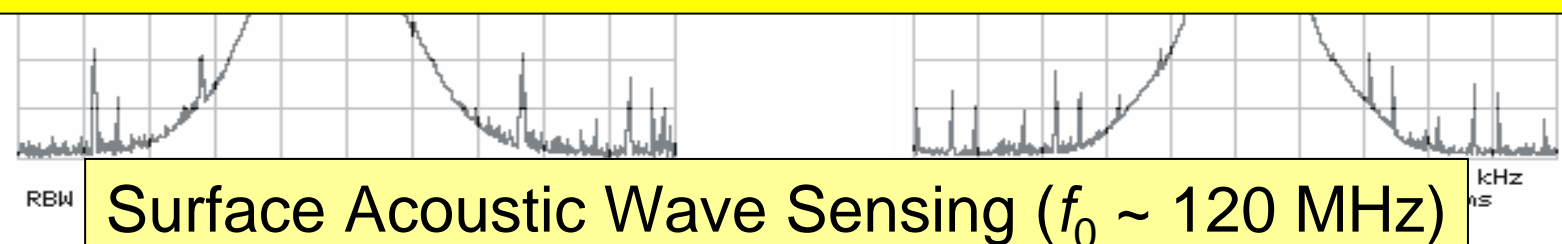
- 1. Au nanoparticles formed by the reduction of AuCl₄⁻ with trisodium citrate are **negatively charged** because of the adsorption of anion species.
- 2. APTMS-monolayer-covered surface is terminated by the **protonated amino group** (NH₃+).



Au nanoparticles used as:

- Nanosized mass standards for quantitative SAW detection
- Mass amplification tags with functionalized ligands

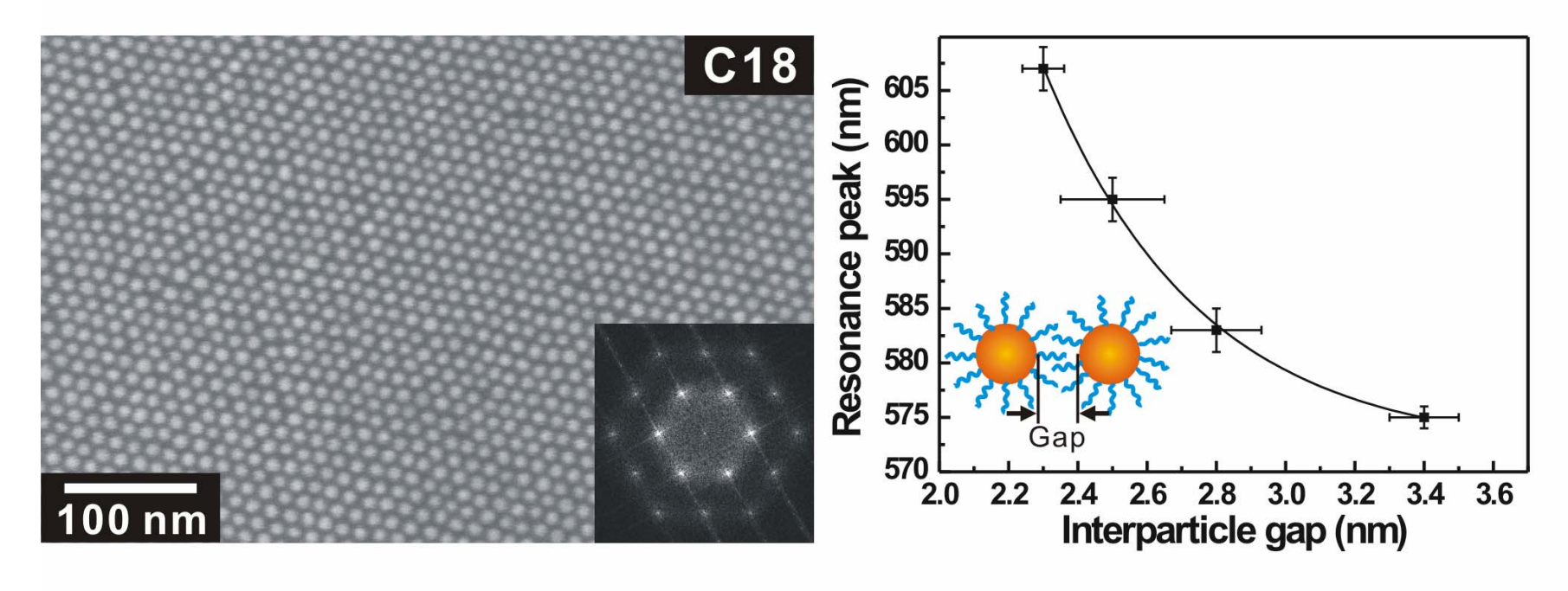
Published in Analytical Chemistry



Tunable Plasmonic Response from Alkanethiolate-Stabilized Gold Nanoparticle Superlattices: Evidence of Near-Field Coupling



Chi-Fan Chen,[†] Shien-Der Tzeng,[‡] Hung-Ying Chen,[†] Kuan-Jiuh Lin,[‡] Shangjr Gwo*,[†]

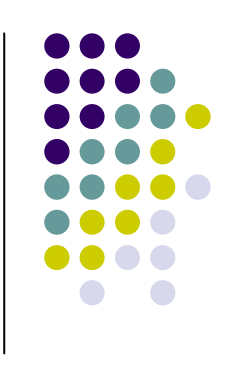


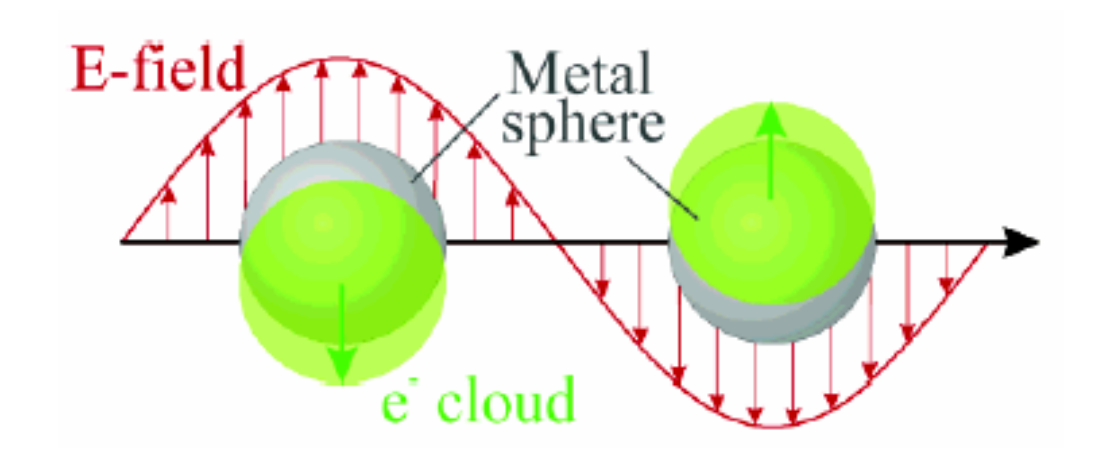
ABSTRACT

We report on the self assembly of large-area, highly-ordered 2D superlattices of alkanethiolate-stabilized gold nanoparticles (~10.5 nm in core diameter) onto quartz substrates with varying lattice constants, which can be controlled by the alkyl chain lengths, ranging from C12 (1-dodecanethiolate), C14 (1-tetradecanethiolate), C16 (1-hexadecanethiolate), to C18 (1-octadecanethiolate). These 2D nanoparticle superlattices exhibit strong collective surface plasmon resonance that is tunable via the near-field coupling of adjacent nanoparticles. The approach presented here provides a unique and viable means of building artificial "plasmonic crystals" with precisely designed optical properties, which can be useful for the emerging fields of plasmonics, such as subwavelength integrated optics.

To appear in JACS (Communication)

Localized Surface Plasmon Resonance





$$m_{\rm e} \frac{\mathrm{d}^2 x}{\mathrm{d}t^2} + m_{\rm e} \Gamma \frac{\mathrm{d}x}{\mathrm{d}t} + Kx = e \mathbf{E}$$

Schematic of plasmon oscillation for a sphere, showing the displacement of the conduction electron charge cloud relative to the nuclei.

$$x = \frac{e\mathbf{E}}{m_{\rm e}(\omega_{\rm R}^2 - \omega^2 - i\Gamma\omega)}$$

K. L. Kelly, E. Coronado, L. L. Zhao, and G. C. Schatz,

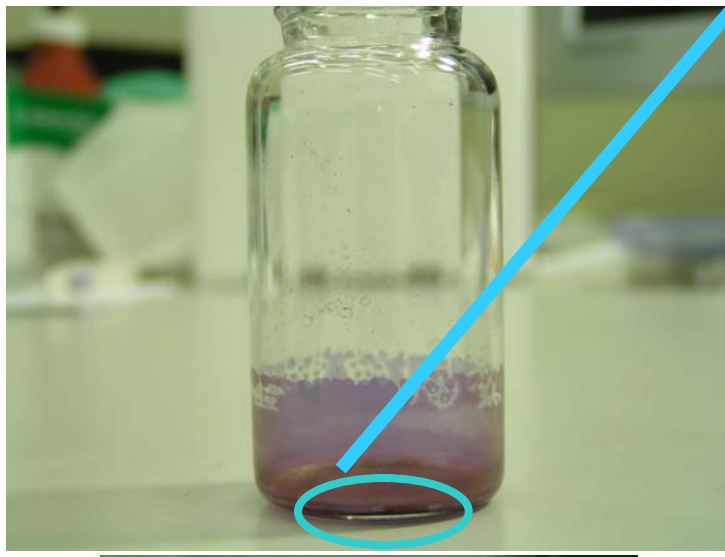
J. Phys. Chem. B 2003, 107, 668-677

Gold Nanoparticles

Lycurgus cup in the period of Byzantine Empire (4th century A.D.) is the most famous glass cup which utilized colloidal metals to fabricate ruby glass.











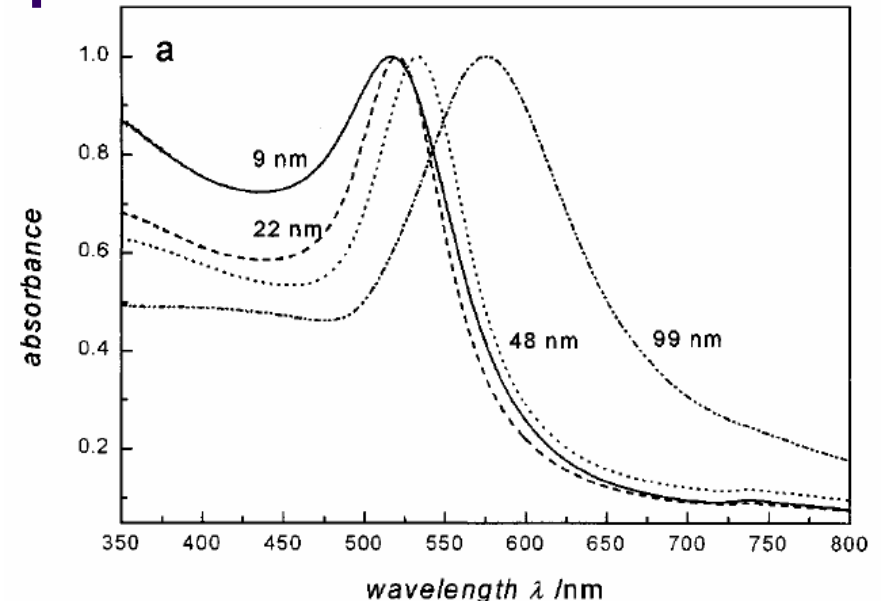


The Lycurgus cup appears to be ruby red in the transmitted light, but exhibits a green color in the reflected light.

S. A. Maier and H. A. Atwater, Journal of Applied Physics 98, 011101 (2005)

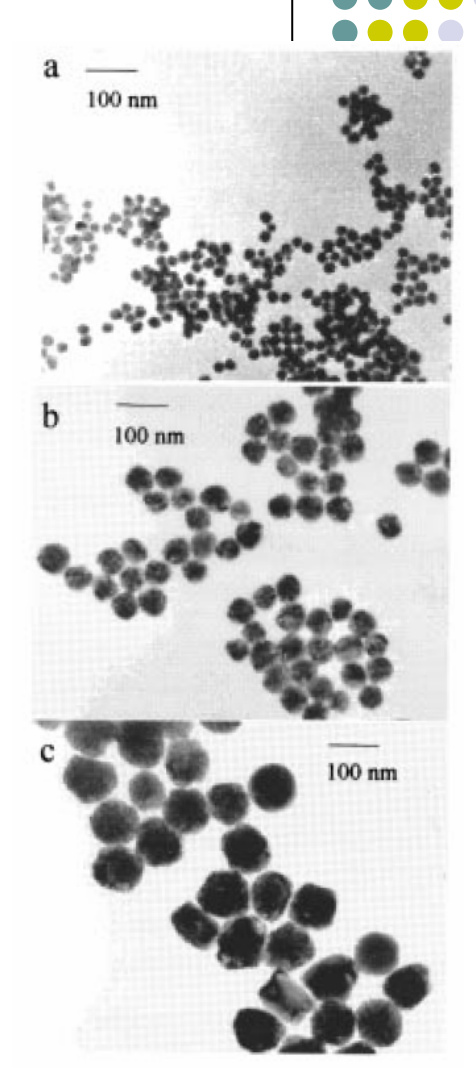
Localized surface plasmon band is sensitive to nanoparticle composition, size, shape, and local dielectric environment.

Size Dependence of the Plasmon Absorption of Colloidal Gold Nanoparticles



UV-vis absorption spectra of 9, 22, 48, and 99 nm gold nanoparticles in water. All spectra are normalized at their absorption maxima, which are 517, 521, 533, and 575 nm, respectively.

S. Link and M. A. El-Sayed, *J. Phys. Chem. B* **1999**, *103*, 4212-4217.



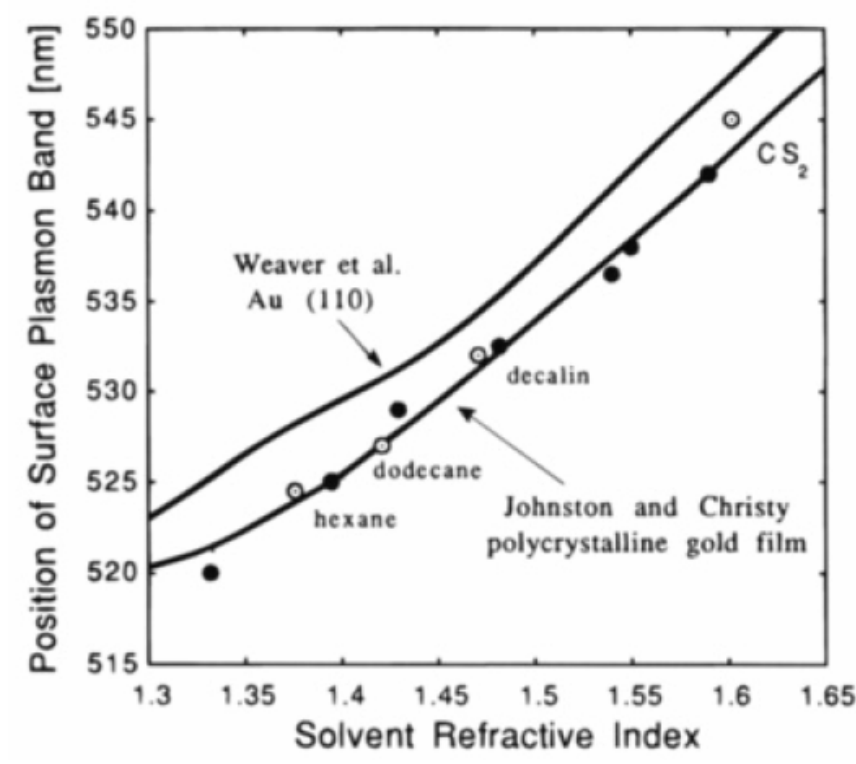
TEM images of the 22 (a), 48 (b), and 99 nm (c) gold nanoparticles

Effect of the Solution Refractive Index on the SPR Band of Gold Colloids





Photograph of five sols of colloidal gold prepared in water and in mixtures of butyl acetate and carbon disulfide. Refractive indices of the solutions at the absorption band maximum are 1.336, 1.407, 1.481,

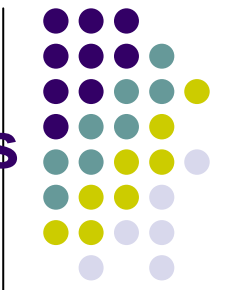


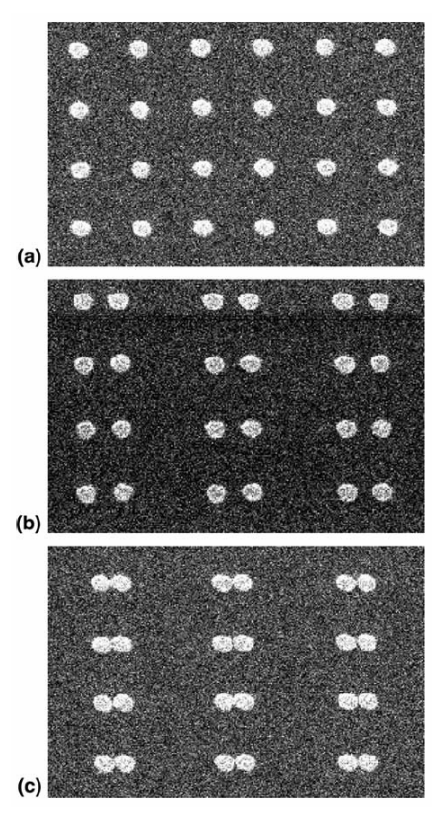
Measured position of the surface plasmon band of colloidal gold as a function of the solvent refractive index for mixtures of butyl acetate and CS₂. The theoretical curves were calculated.

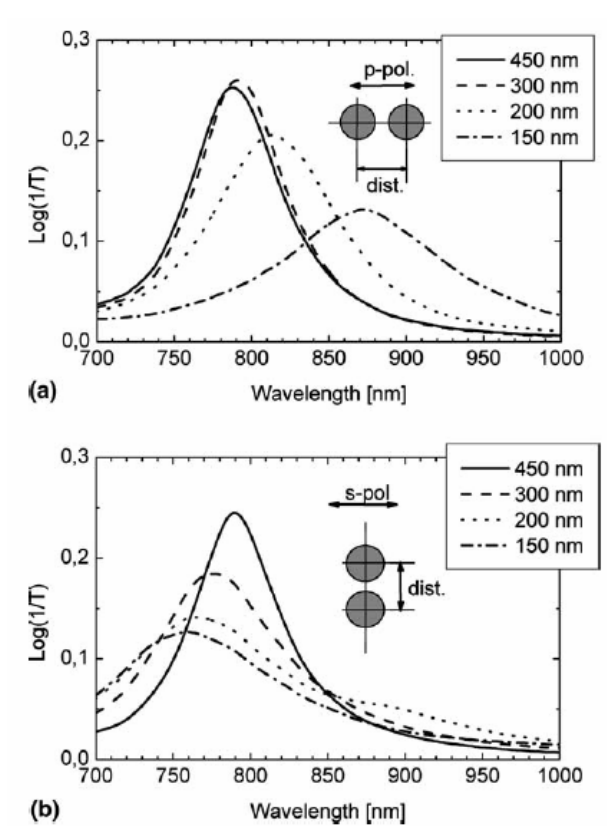
1.525, and 1.583 respectively.

S. Underwood and P. Mulvaney, *Langmuir* **1994**, *10*, 3427-3430.

Optical properties of two interacting gold nanoparticles





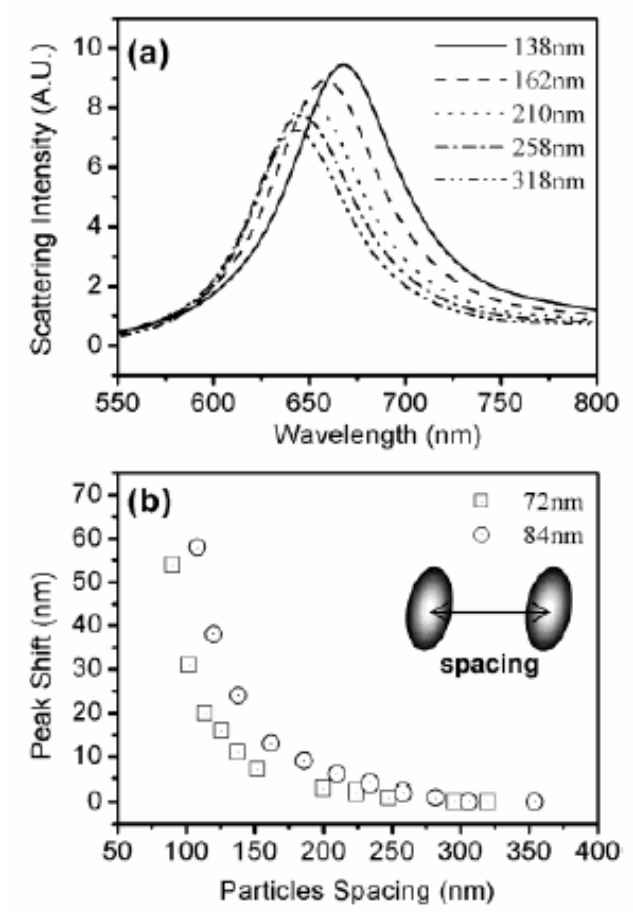


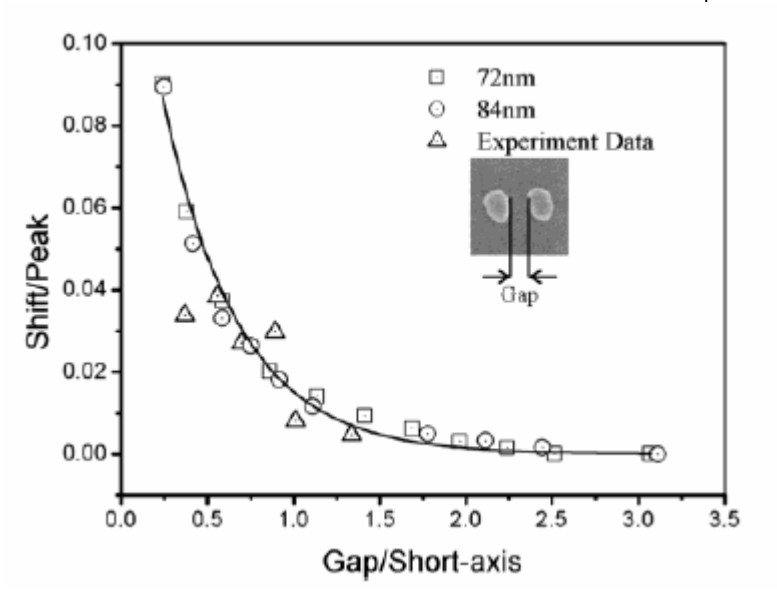
Extinction spectra of a 2D array of the Au nanoparticle pairs with the interparticle center-tocenter distances as the parameter. The polarization direction of the exciting light is (a) parallel to the long particle pair axis and (b) orthogonal to it.

SEM images of particle pair samples with varying interparticle distance (center-to-center) of (a) 450 nm, (b) 300 nm and (c) 150 nm. The particle diameter is 150 nm, the particle height is 17 nm.

W. Rechberger, A. Hohenau, A. Leitner, J. R. Krenn, B. Lamprecht, F. R. Aussenegg, *Optics Communications* **2003**, *220*,137–14.

Interparticle coupling effects on SPR of gold nanoparticle pairs





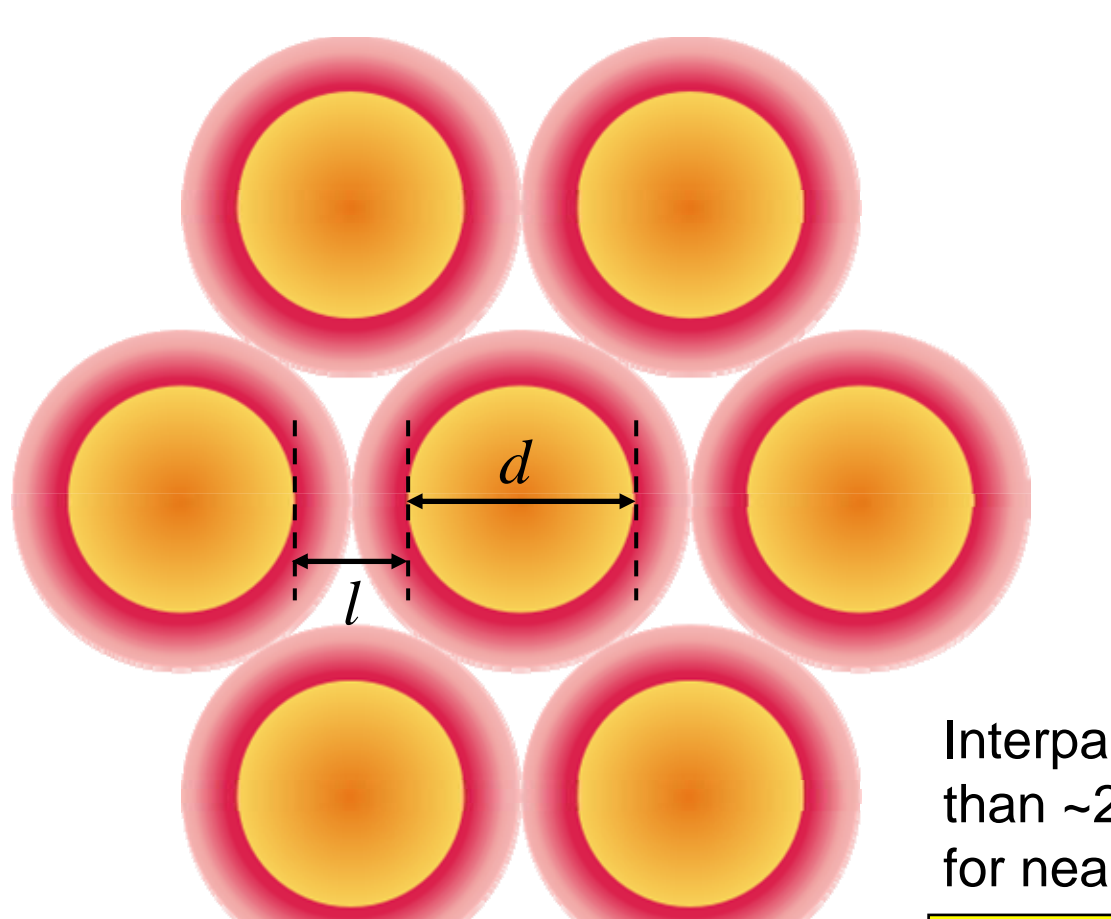
Comparison of computer-simulated (\square , O) and experimentally \triangle measured resonant wavelength shifts as a function of the gap between two particles.

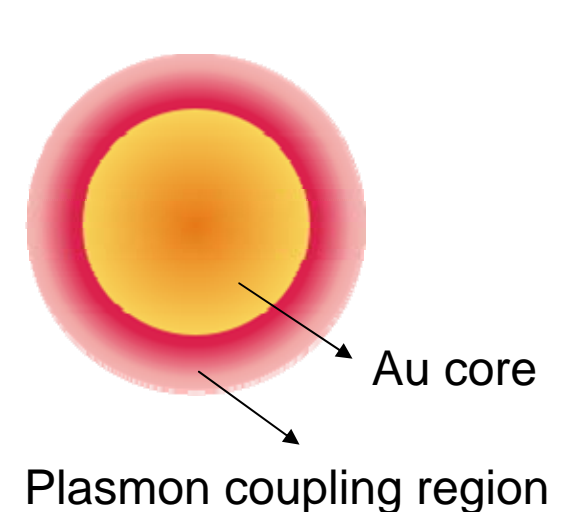
(a) Simulated scattering spectra of two coupled Au elliptical disks. The short axis is kept at 84 nm. The center-center particle spacing is varied from 138 to 318 nm. (b) Resonant-peak wavelength as a function of particle center-center spacing for particles with short-axis lengths of 72 and 84 nm.

K.-H. Su, Q.-H. Wei, X. Zhang, J. J. Mock, D. R. Smith, and S. Schultz, *Nano Lett.* **2003**, *3*, 1087-1090.

Difficulty of realizing near-field coupled SPR from Au nanoparticles superlattices (Tunable plasmonic crystal, Collective SPR)



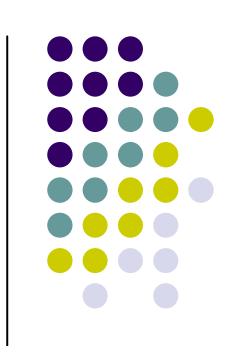


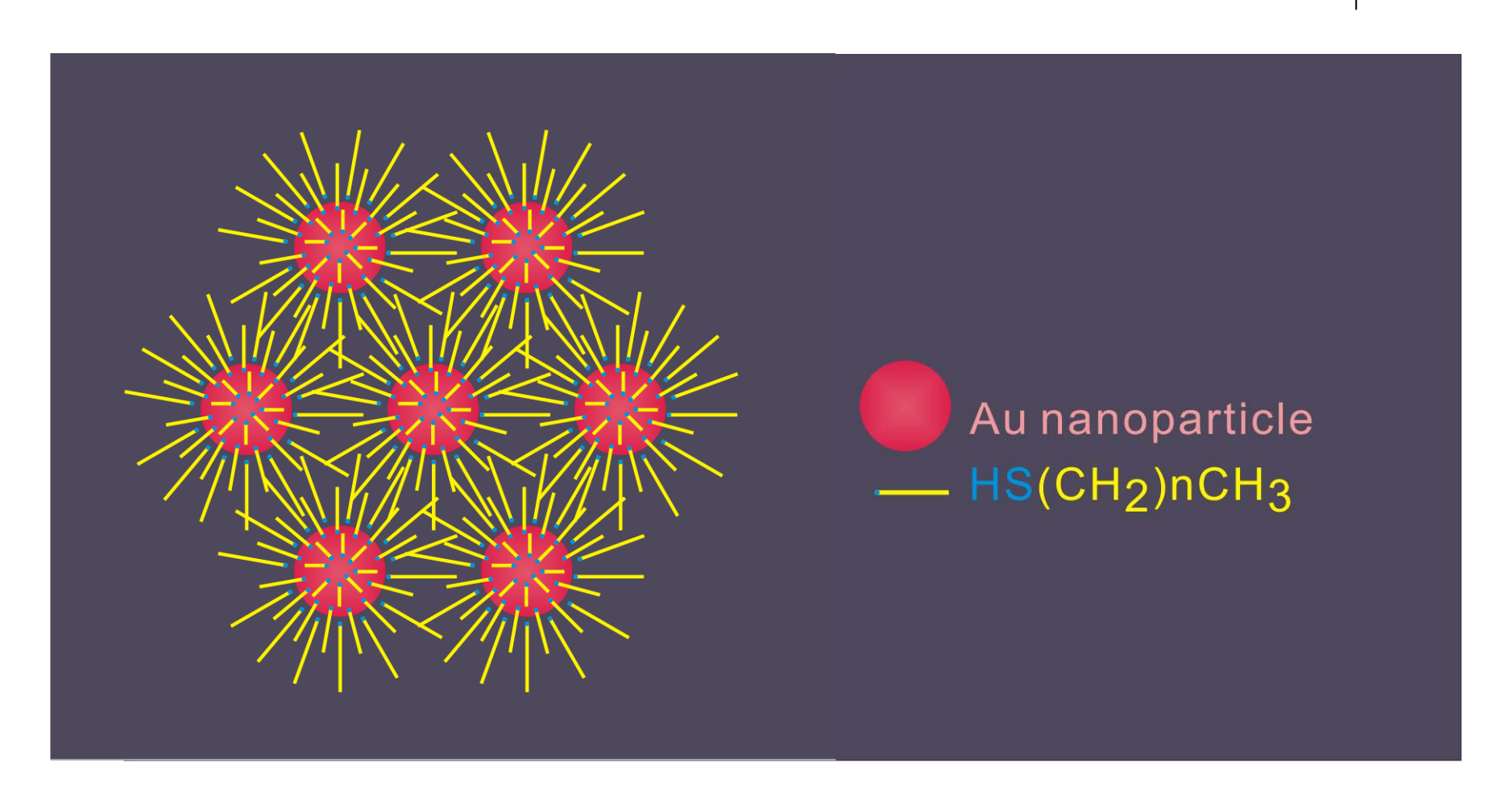


Interparticle distance should be less than ~20% of the nanoparticle diameter for near-field coupling effect

For 10 nm Au nanoparticles l < 2 nm!

Close packed alkanethiolate-stabilized Au nanoparticles





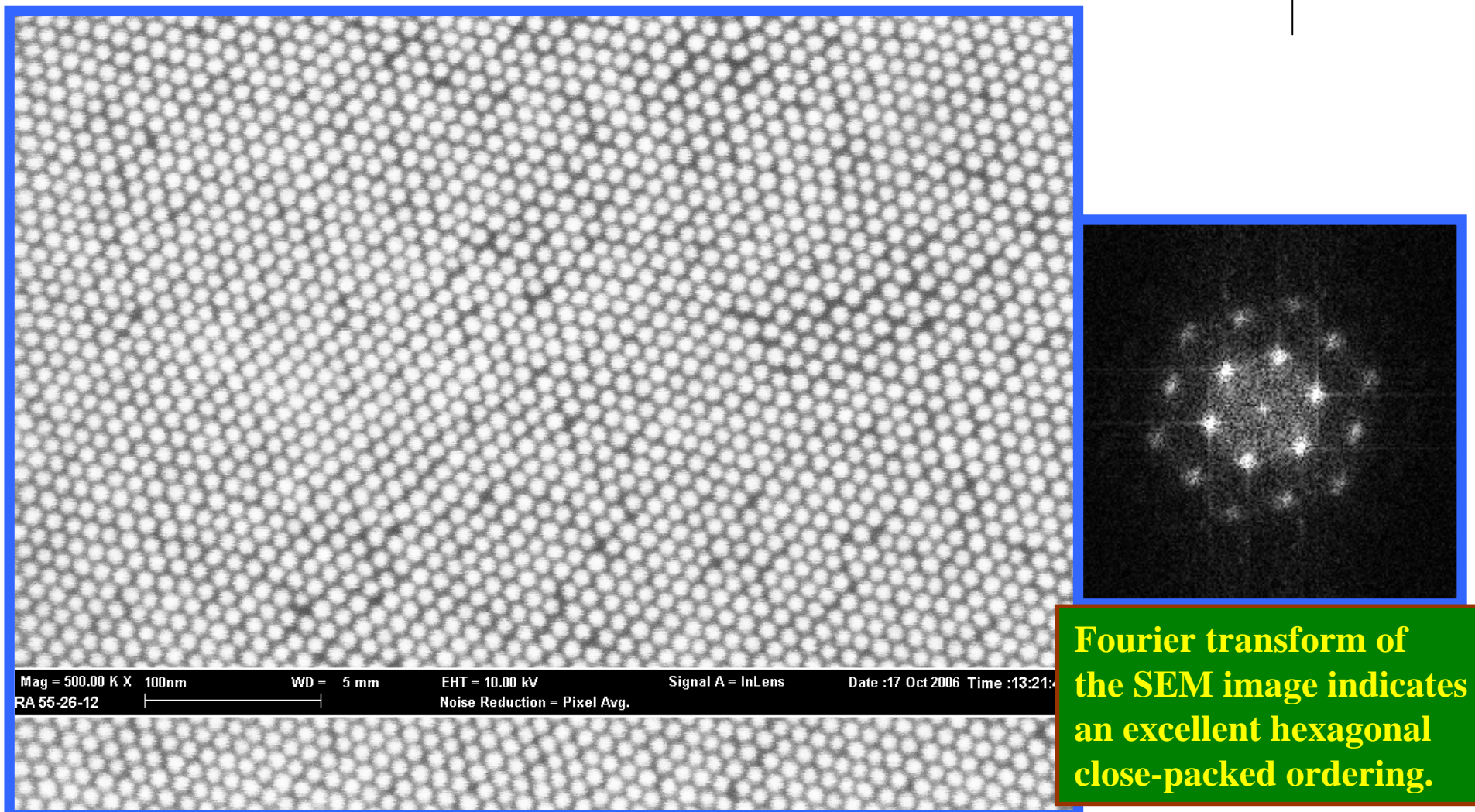
Road Blocks to be Cleared for Synthesizing Au@thiolate nanoparticle superlattices

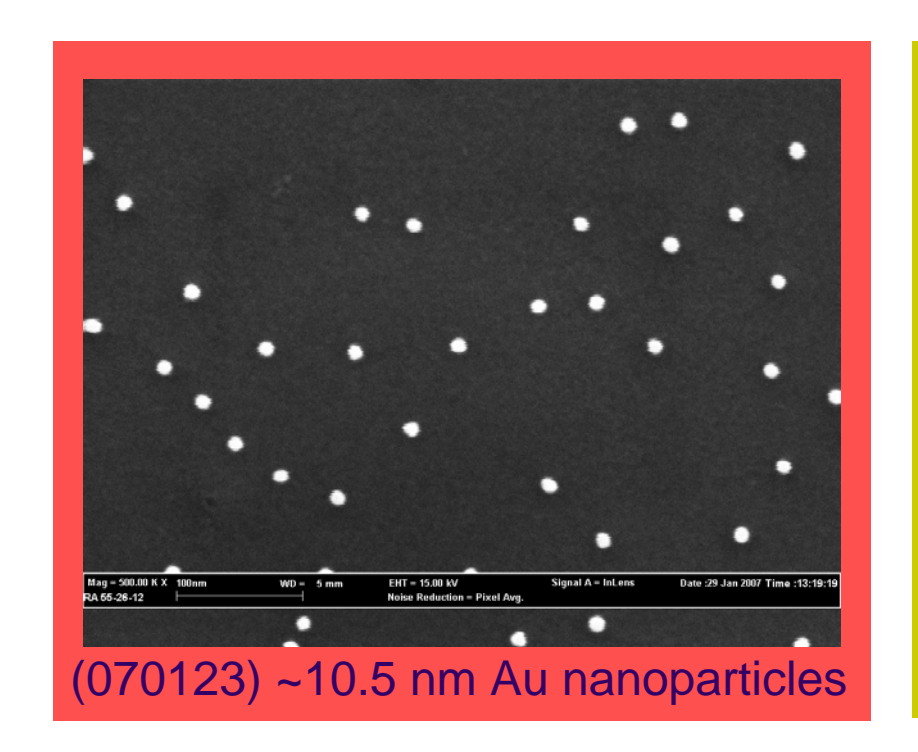


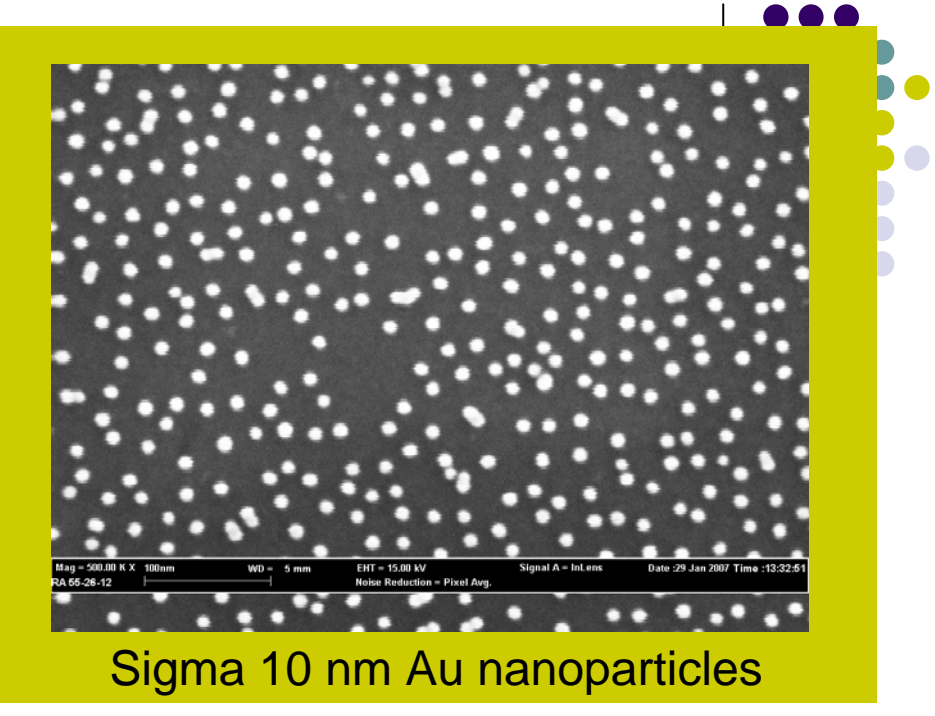
- ➤ Nanoparticle size limit
- In the presence of thiols, typical $d_{Au} \leq 5$ nm (plasmon damping coefficient is too high!)
- → Modified two-step, two-phase method
- → Up to 15 nm in nanoparticle diameter
- **➤**Uniform core size with different alkyl lengths
- → C12, C14, C16, C18
- ▶ Large superlattice size
- \rightarrow Up to 1×1 mm² of long range ordering
- >Transparent substrates
- → Self assembly on quartz substrates
- → Solutions for SEM imaging / optical absorption measurement

2D close-packed 10 nm Au nanoparticles modified with dodecanethiol (Chi-Fan Chen)



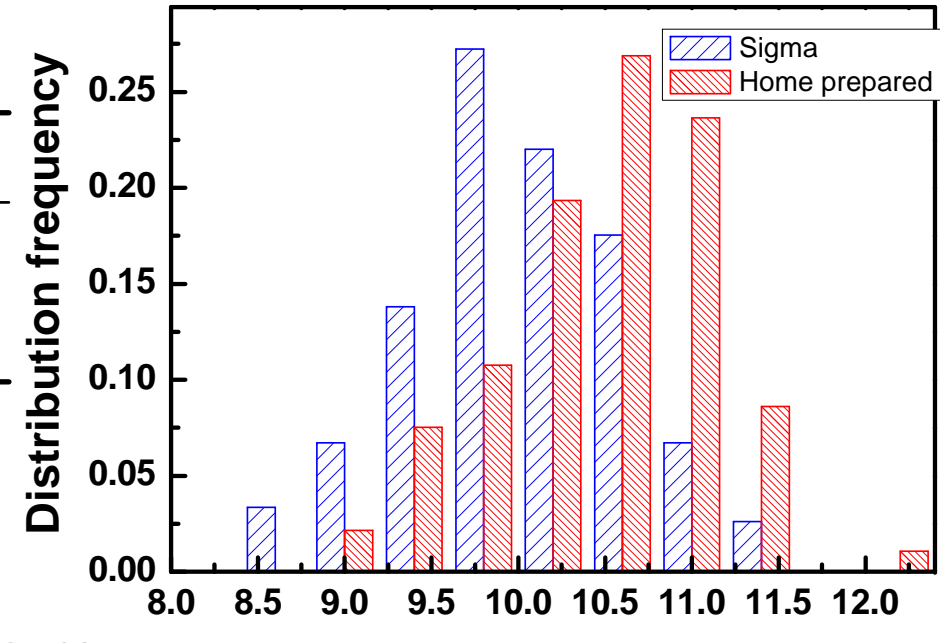






Sample	Mean Diameter (nm)	Standard Deviation (nm)	Standard Deviation (%)
Au colloids (Sigma)	10	0.6	6%
Au colloids (prepared by us)	10.5	0.6	5.8%

The mean diameter and size distribution of gold colloids dispersed in water.

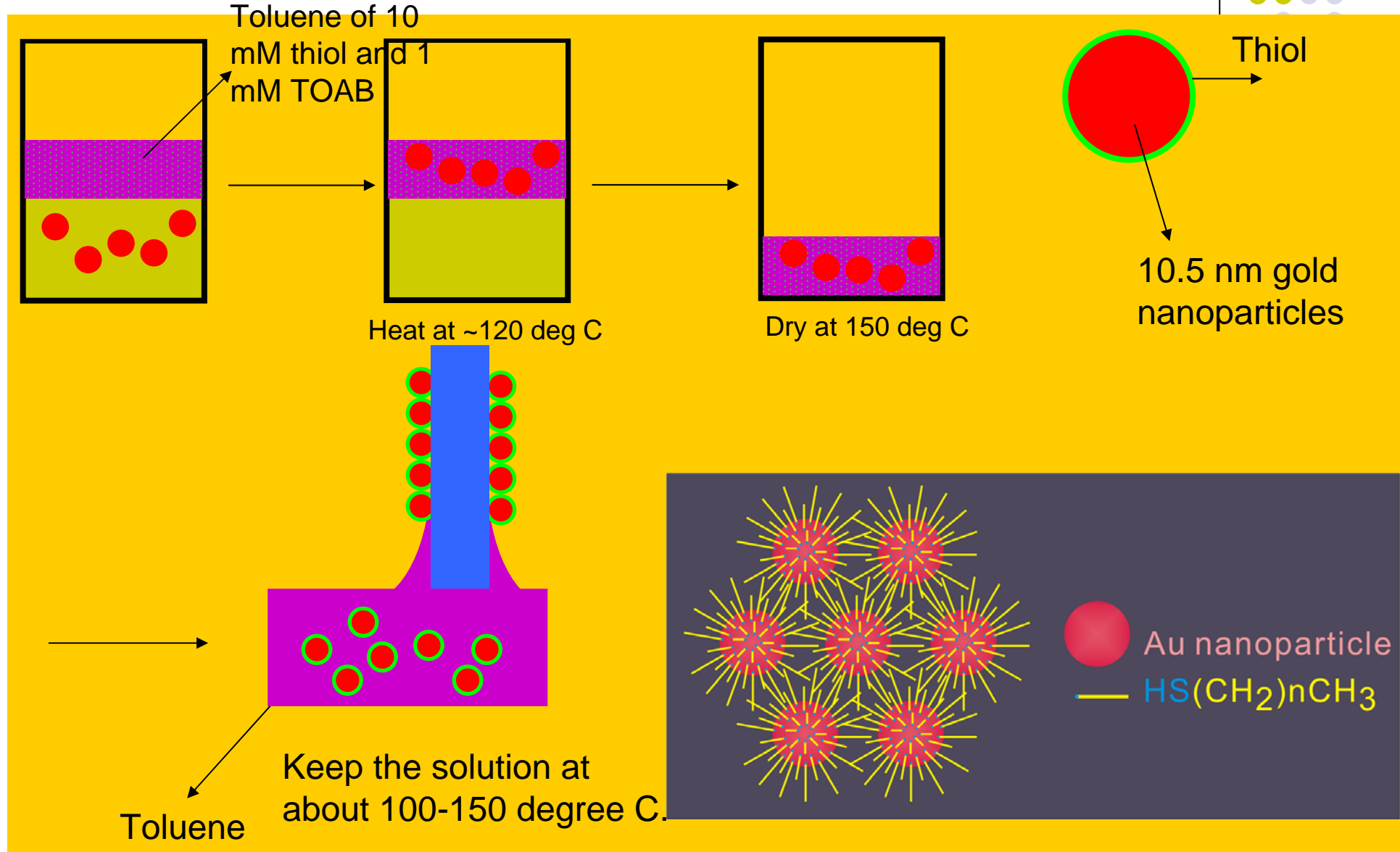


Particle diameter (nm)

J. W. Slot and H. J. Geuze, Eur. J. of Cell Biol. 1985, 38, 87-93.

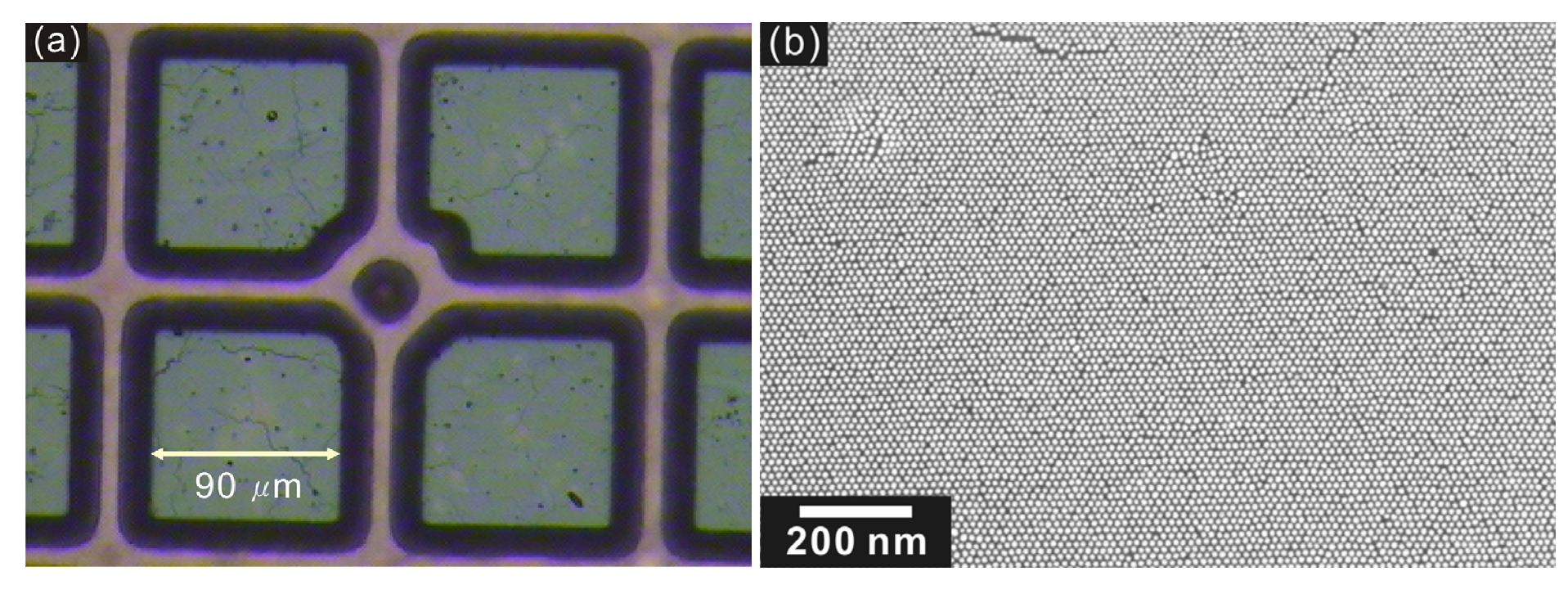
Self-assembly Au superlattices onto quartz substrates



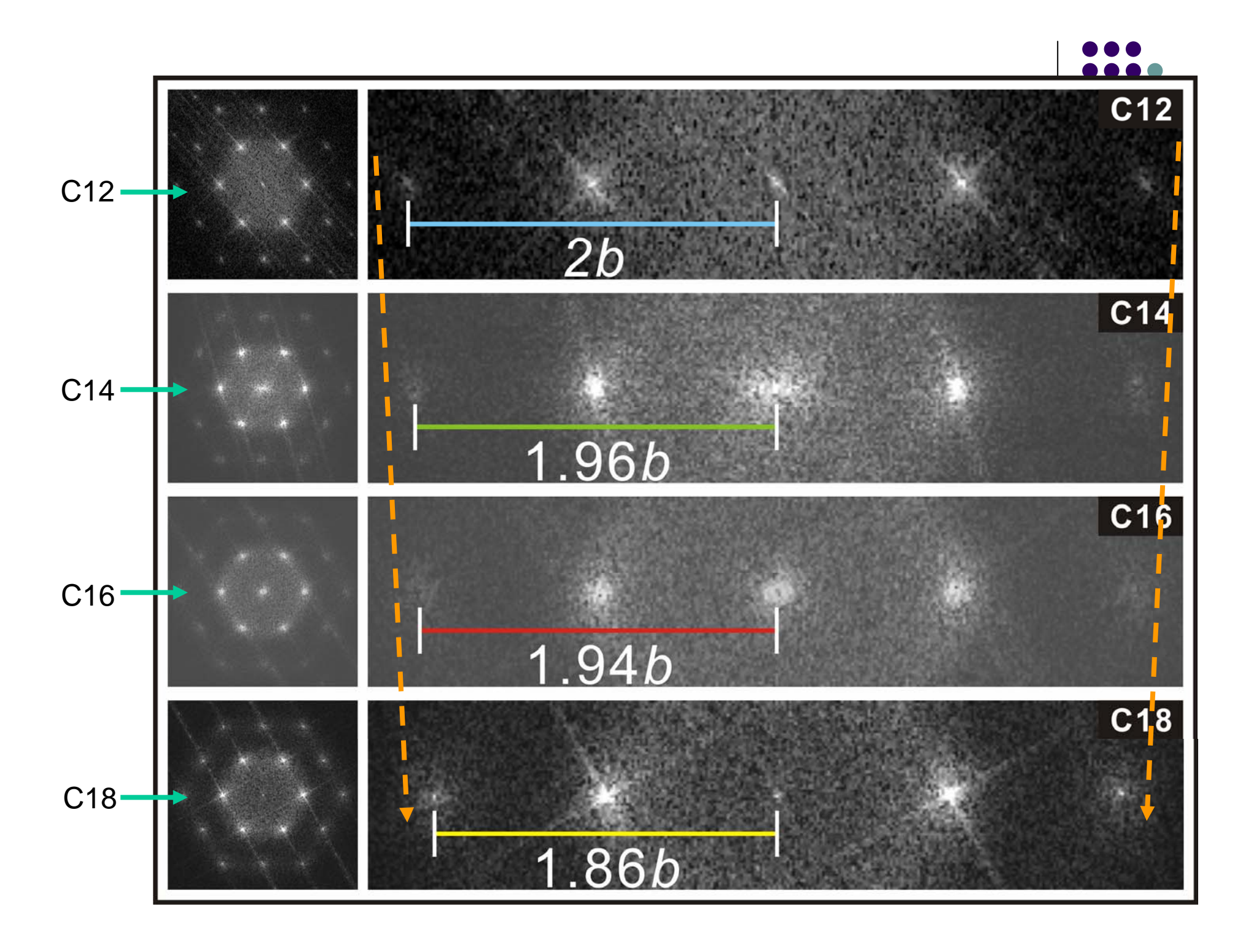


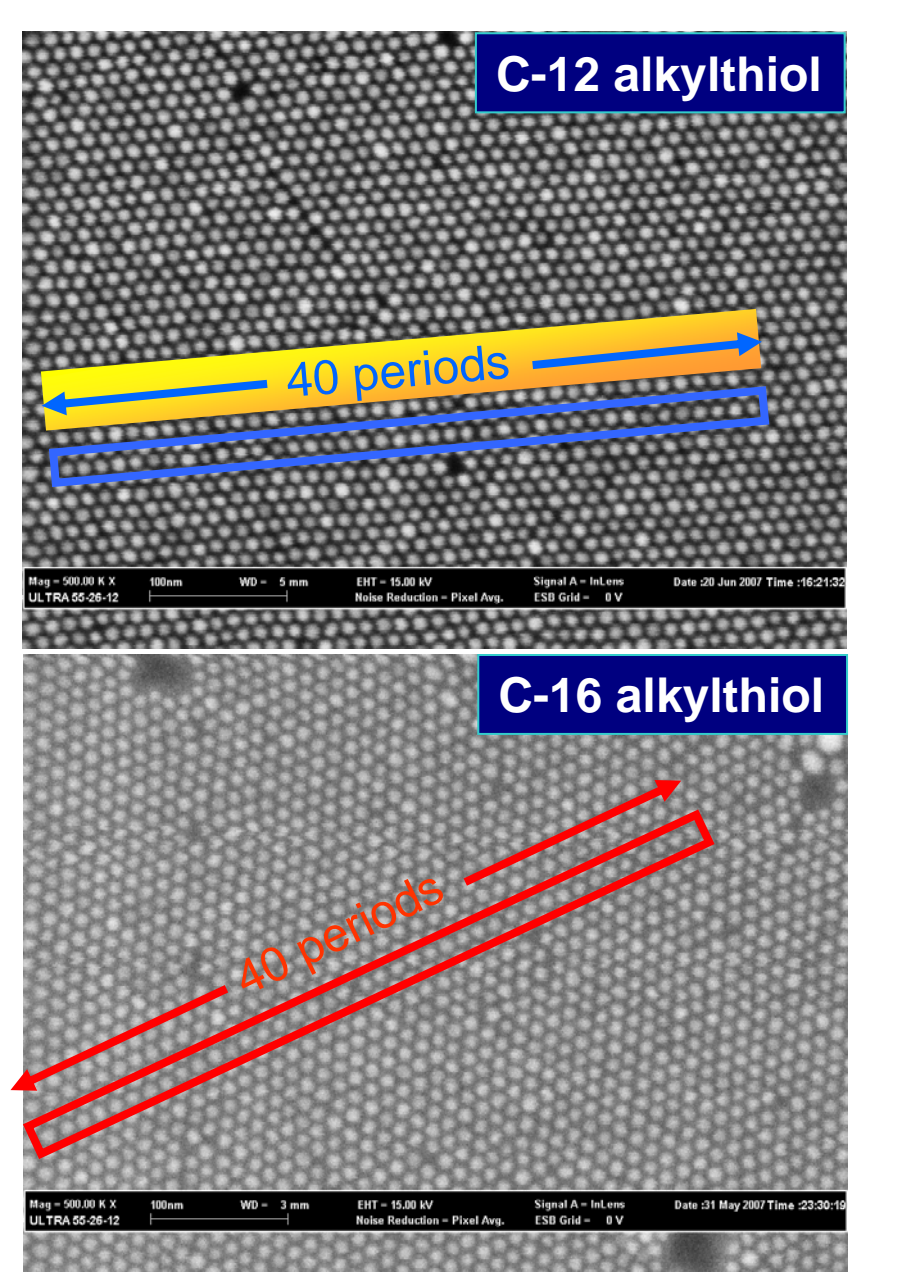
Optical microscope image/SEM image of Au@c18 nanoparticles superlattice

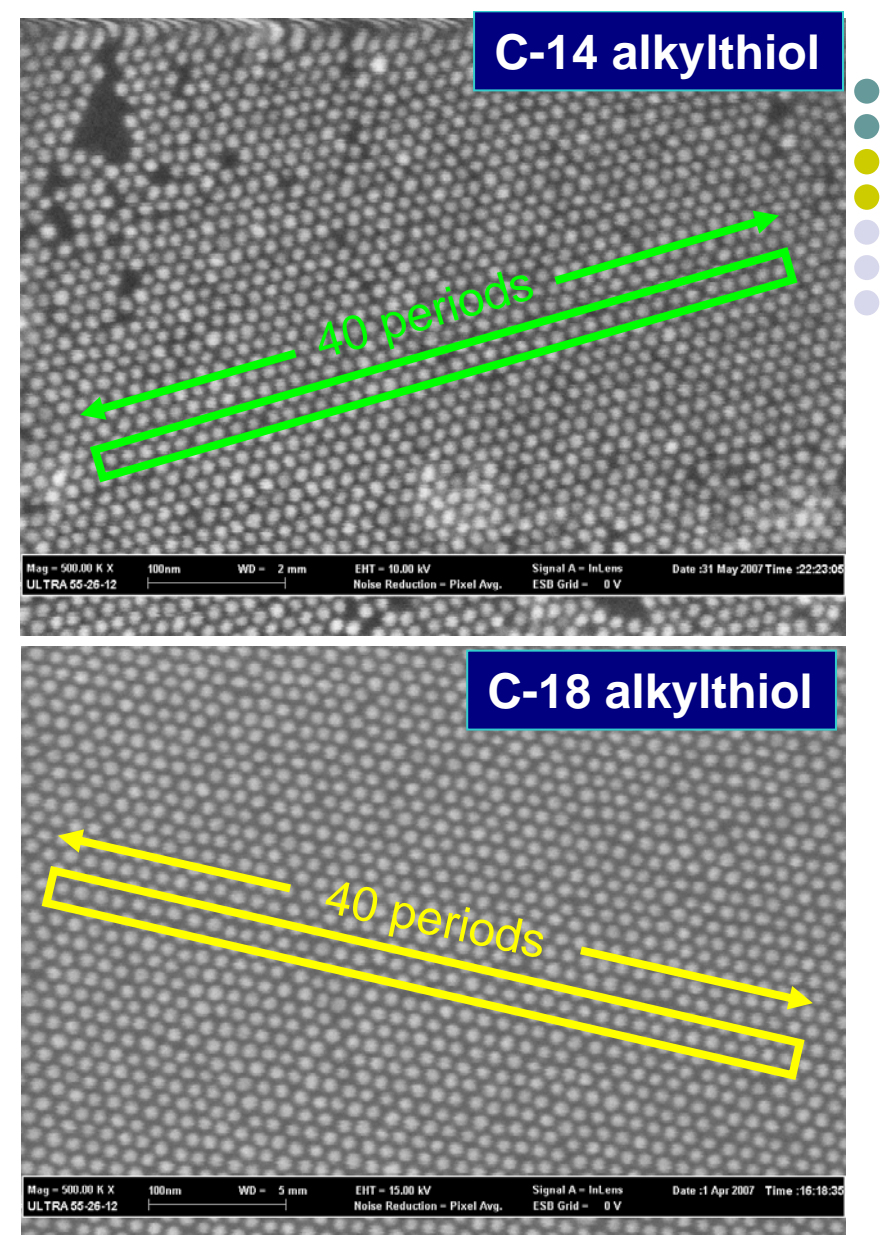


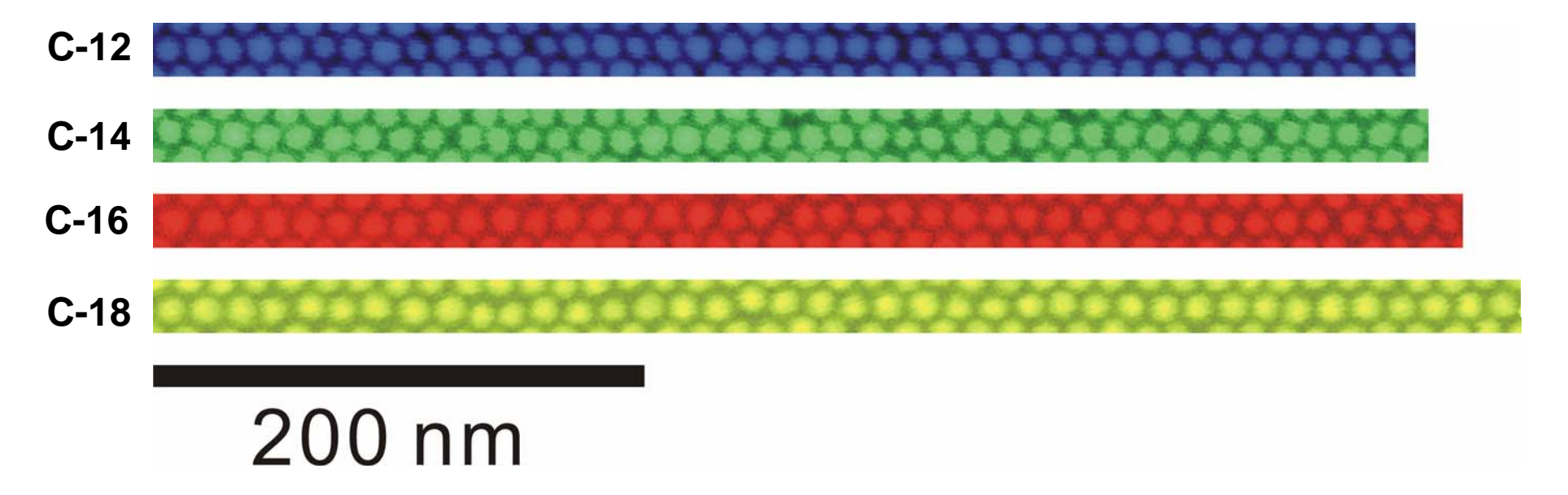


(a) Optical microscope image of the closely packed 2D superlattice of octadecanethiolate-stabilized gold nanoparticles (Au@C18) on the quartz surface. The self-assembled Au@C18 nanoparticle superlattice is highly ordered and its spatial extension can exceed 1×1 mm².. (b) FE-SEM image of the Au@C18 closely packed nanoparticle superlattice on quartz with an imaging area of $1\times1.5~\mu\text{m}^2$.





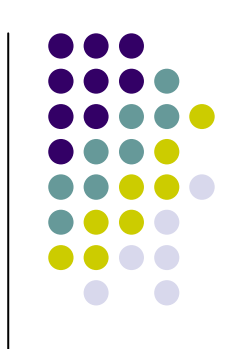


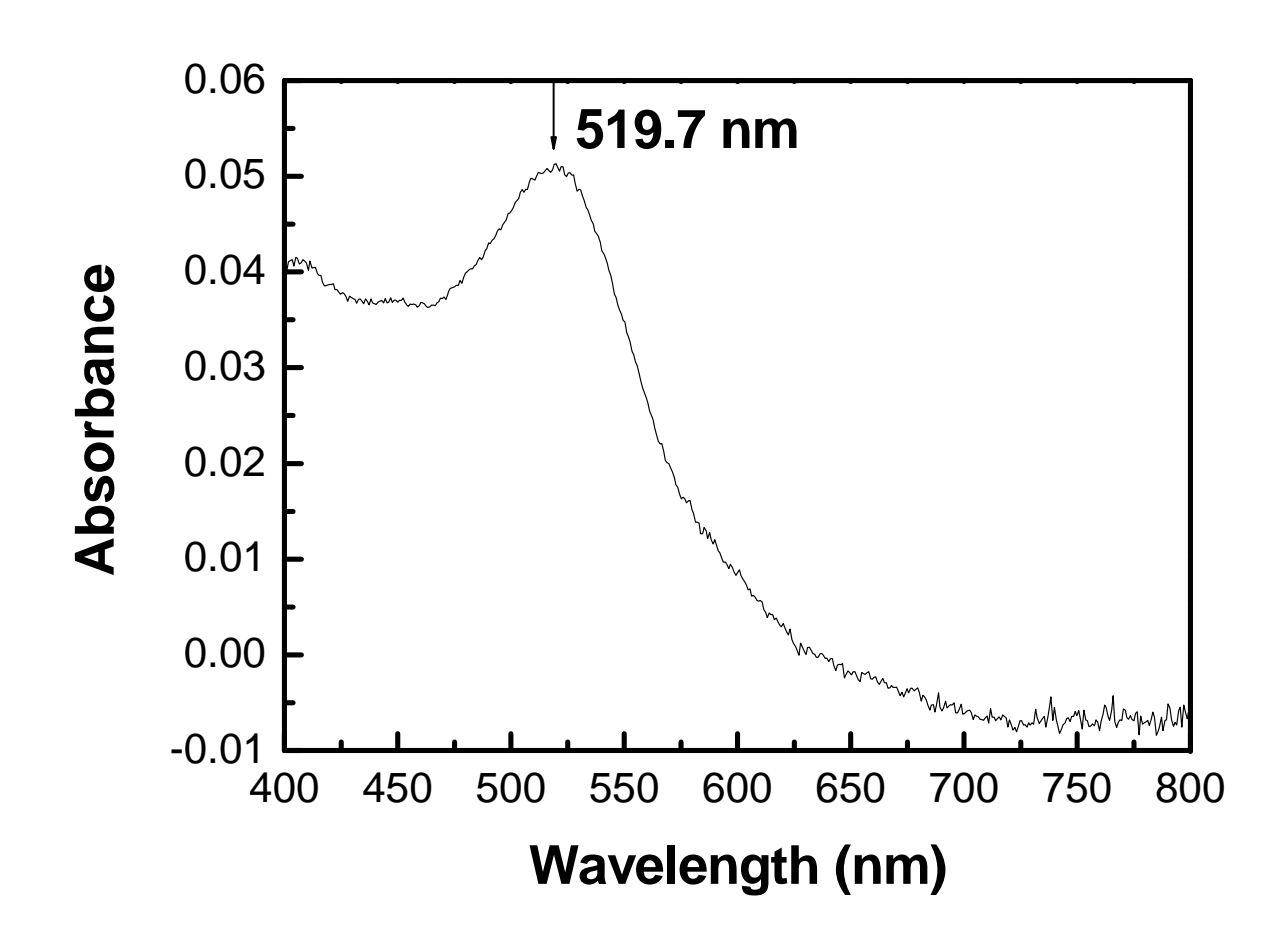


Sample	Average Period (nm)	Standard Deviation (nm)	Standard Deviation (%)	Inter- Particle Gap (nm)	Gap/Dia- meter
C12-Au	12.8	0.06	0.4 %	2.3	0.22
C14-Au	13.0	0.15	1.2 %	2.5	0.24
C16-Au	13.3	0.13	1.0 %	2.8	0.27
C18-Au	13.9	0.10	0.7 %	3.4	0.32

Summary of the main results obtained from hexagonal close-packed, alkanethiolate-stabilized Au nanoparticle superlattices.



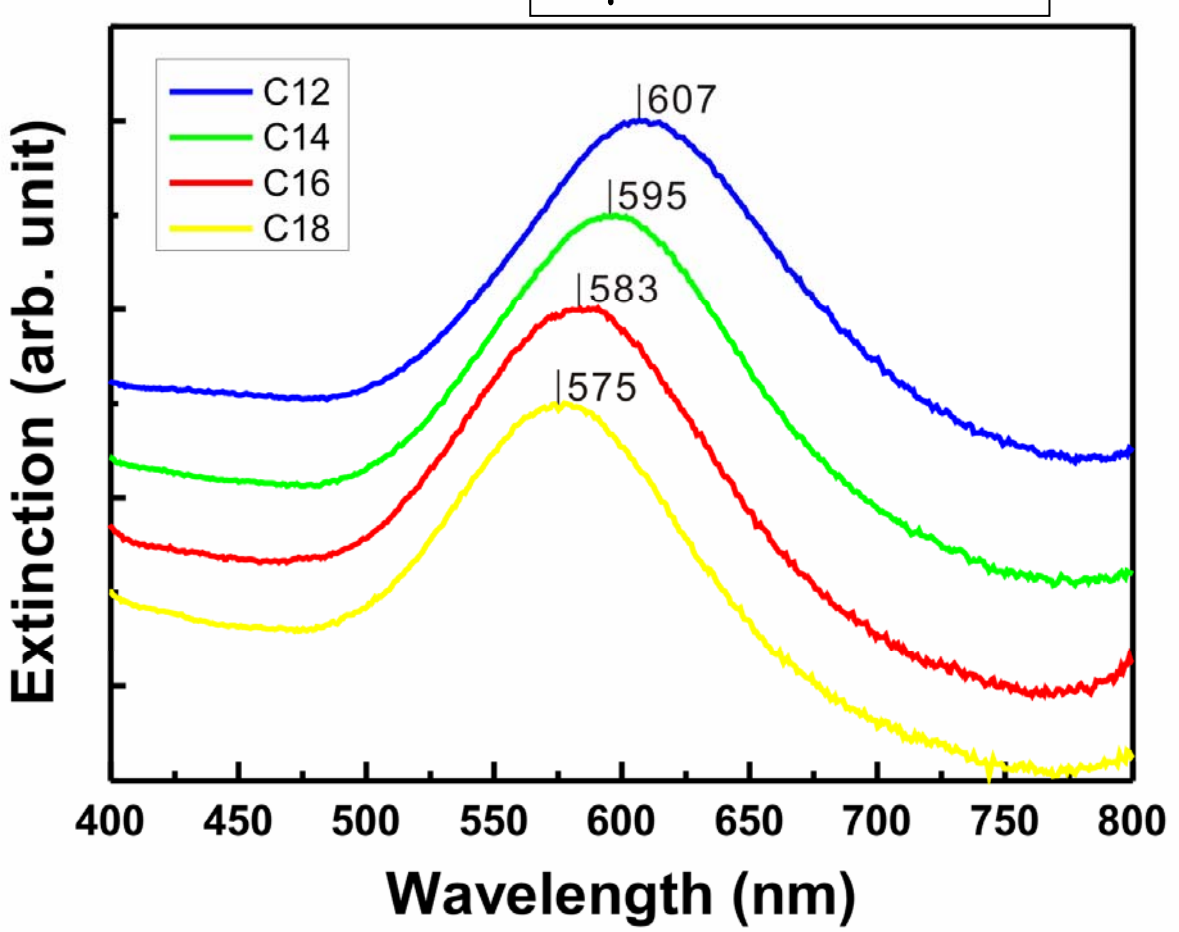




Au nanoparticle superlattices whose periods are tuned by different length of alkylthiol result in red shift of collective

surface plasmon band

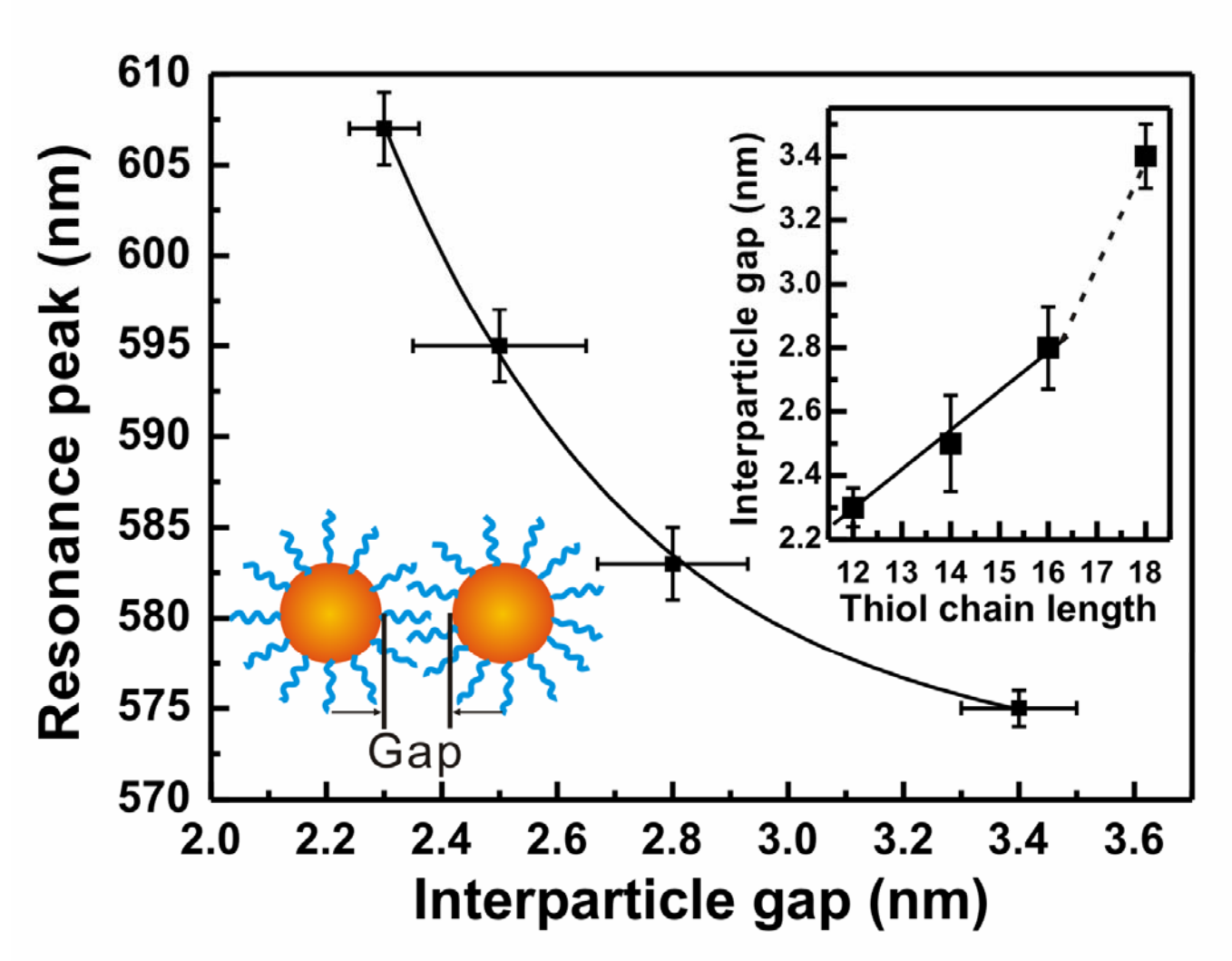
Probing area: 7 μm in diameter





Collective plasmon resonance peak as a function of the interparticle gap



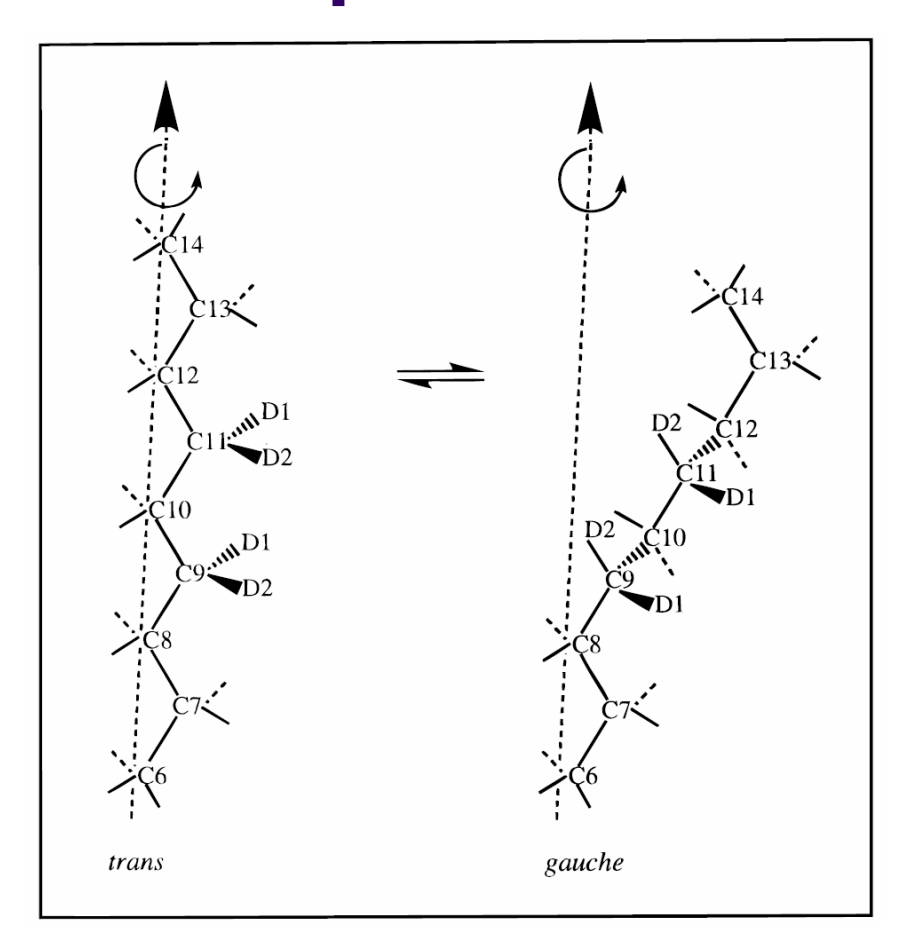


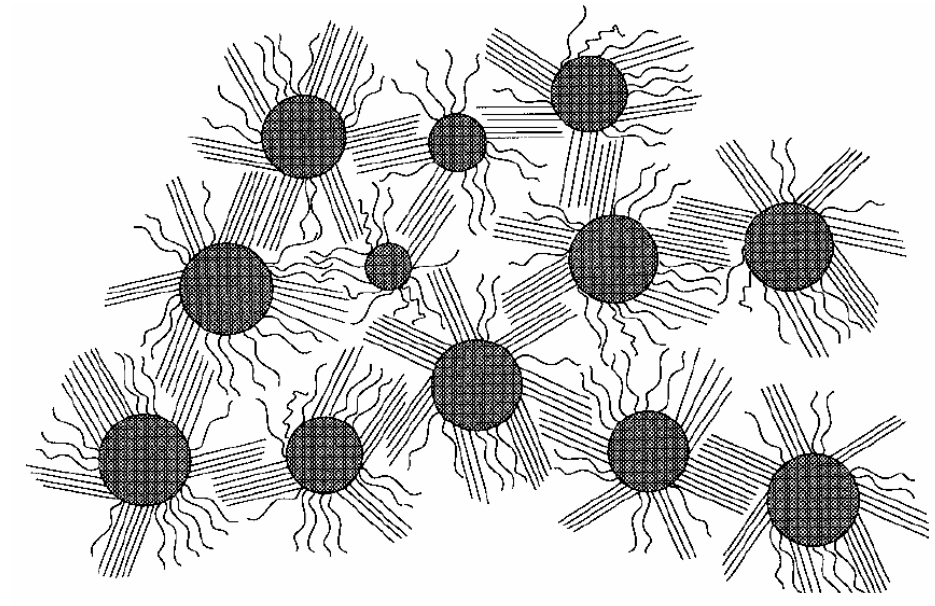
$$l = 0.83 + 0.122n$$

where n is the number of carbon atoms per chain and l is the interparticle gap

Order-Disorder Transition of Thiol SAMs on Nanoparticles



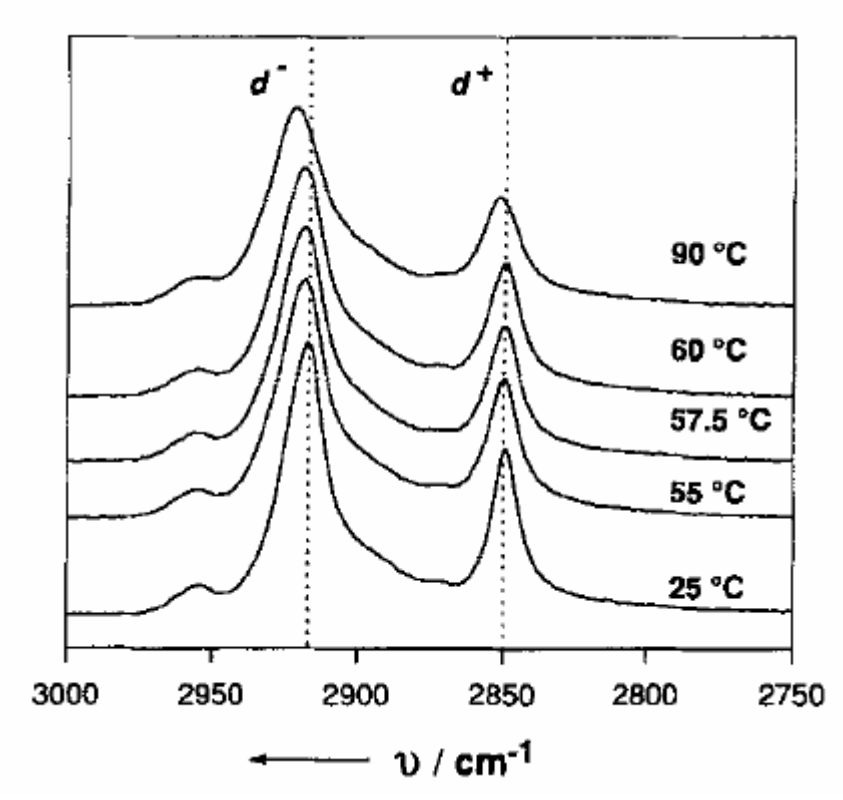




^a In this description, *domains* or *bundles* of ordered alkylthiolate chains on a given Au particle will interdigitate into the chain domains of neighboring particles in order to compensate for the substantial decrease in the chain density which occurs toward the methyl chain end. Chains with large populations of *gauche* bonds may arise from (i) those which occupy interstitial regions in the particle lattice and cannot efficiently overlap with adjacent chains or from (ii) chains residing at domain boundaries.

A. Badia, L. Cuccia, L. Demers, F. Morin, and R. B. Lennox, *J. Am. Chem. Soc.* **1997**, *119*, 2682-2692.

orientation of thiol SAMs on planar gold.[15] However, the dispersed nature of the gold nanoparticle system allows us to use conventional transmission FT-IR, with the sample deposited as a thin film on an inert substrate. For example, Figure 5 tracks the CH₂ symmetric (d^+ : 2850 cm⁻¹) and antisymmetric (d^- : 2920 cm⁻¹) stretches of C₁₈S-Au as a function of temperature. Figure 6 thus shows that upon heating, the C₁₄S-, C₁₆S-, and C₁₈S-Au samples undergo a transition from a highly chainordered state to a chain-disordered state, where the CH, symmetric $(d^+: 2850 \text{ cm}^{-1})$ and antisymmetric $(d^-: 2920 \text{ cm}^{-1})$ stretches are used as markers of trans and gauche bond populations in the chains. [2, 16] Although this process occurs over a relatively broad temperature range (≈25 °C), as is the case in the NMR and calorimetry experiments (Figs. 3 and 4), the apparent transition temperatures are similar to those found by other techniques reported here. Also notable is the observation that the population of gauche bonds at 25°C follows the trend of $C_{14} > C_{16} > C_{18}$. This is consistent with a differing extent of



Variable-temperature transmission FT-IR spectra of the CH, stretching region (2750-3000cm-') for C,,S-Au particles. The dotted lines at 2917 and 2850 are visual aids.

A. Badia, S. Singh, L. Demers, L. Cuccia,G. R. Brown, and R. B. Lennox, *Chem. Eur. J.* **1996**, *2*, 359-363.

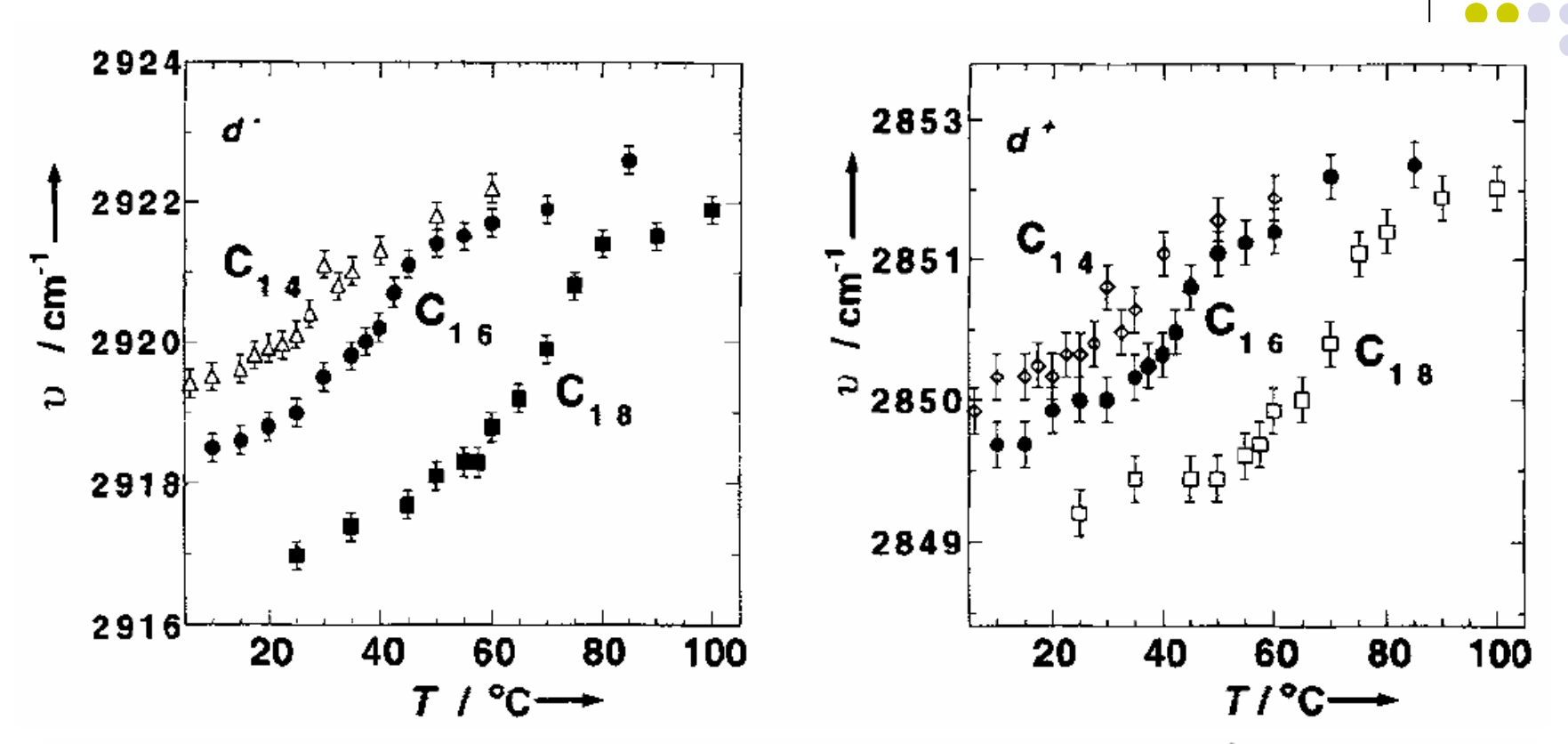
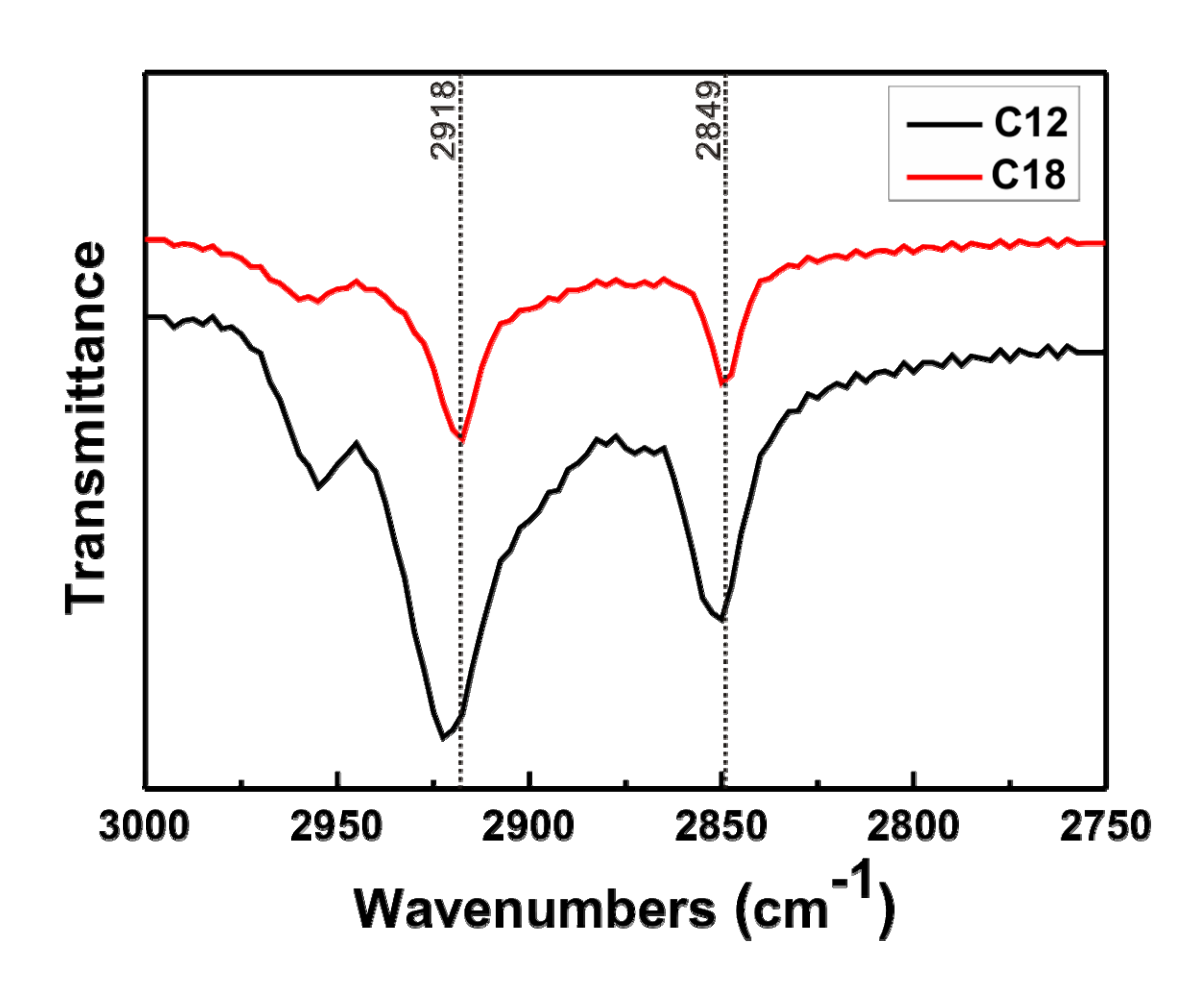


Fig. 6. Peak position of the antisymmetric (d^-) and symmetric (d^+) CH₂ stretches as a function of temperature for RS-Au powders of C₁₄S-, C₁₆S-, and C₁₈S-Au nanoparticles deposited on a NaCl crystal.

A. Badia, S. Singh, L. Demers, L. Cuccia,G. R. Brown, and R. B. Lennox, *Chem. Eur. J.* **1996**, *2*, 359-363.

FT-IR Measurements







Summary:

- We have succeeded in forming Au nanoparticle superlattices with a large ~1×1 mm² superlattice area.
- The period of Au superlattices can be tuned by alkyl chain length with an atomic precision.
- The slight variation of lattice period (atomic scale) could result in a huge shift in the collective plasmon band.
- → A new route for artificial "Plasmonic Crystals" with designed plasmonic properties via tunable near-field coupling